



Full-scale fatigue testing with initial damage as validation of FRP road bridge design

Jan Hiddingh

Provincie Groningen, the Netherlands

Ronald Grefhorst

InfraCore Company, Rotterdam, the Netherlands

Martijn Veltkamp

FiberCore Europe, Rotterdam, the Netherlands

Contact: j.hiddingh@provinciegroningen.nl

Abstract

Bridges built in fibre reinforced polymers (FRP) bring the important advantage of low-maintenance costs, thus reducing the total cost of ownership. Various kinds of FRP-constructions have been built hundreds of times in the last decade, the technology is now beyond the stage of infancy. The Province of Groningen has positive experiences with bridges and lock gates built in FRP. For a 8m span lifting bridge for road usage, the province prescribed FRP as the structural material for the deck, and in parallel required additional validation of the material's fatigue resistance through full-scale testing.

Keywords: Movable bridge; FRP; full-scale testing; impact damage; fatigue.

1 Introduction

In civil engineering FRP is a relatively new material. During the last decade, it is increasingly used in bridges and other civil engineering structures. As a result, frameworks for acceptance and quality assurance are in place or being established in various countries. Due to the relatively small number of FRP structures compared to those built in conventional structural materials and their large geographical spread, these frameworks still have a status of guidance and have not yet reached the status of standards, such as Eurocodes.

In order to progress rather than wait, the road authority of the Province of Groningen (the Netherlands) procured the FRP 'Pijlebrug' in a competitive market, giving room to the material and the FRP supply chain to prove itself. The client has been following the emergence of FRP as a structural material for multiple years, and already commissioned FRP lock gates in 2011. The key reasons for opting for FRP were to:

- obtain a relatively lightweight bridge deck. The architectural design of the bridge left a relatively small space for the counterweights in the towers of the bridge;

- proceed in making FRP a more commonly accepted material in civil engineering, creating greater confidence in the use of FRP;
- actively develop the acceptance of engineering rules or testing of the structure;
- lower maintenance costs.

As each FRP fabricator has its own construction principle, the client decided to leave the responsibility for the design and detail engineering to the (sub)contractor. The client merely made an overall design (Figure 1 and Figure 2) and in addition to the required calculations of the structure, it prescribed a few testing methods in order to prove the proposed construction to meet the requirements

The client as well as the FRP fabricator had a common target in building a product that satisfied the functional requirements and would act as a benchmark for future projects, reducing the need for further testing and validation. Working together mainly on technical solutions fulfilled both needs.

The combination of testing and construction ensured that the tested configuration would be exactly that of what was to be built, with no interpretations required from other types of FRP construction.



Figure 1. The design of the Pijlebrug.

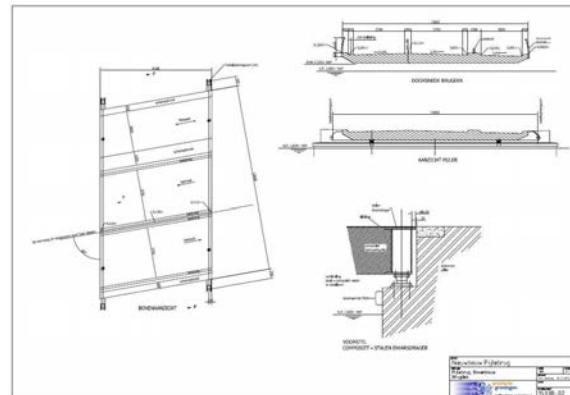


Figure 2. Contract drawing, showing only the overall principles.

2 Tender procedure

For the Pijlebrug, the client had clear ideas about the bridge's functional requirements, and the testing it required to validate the design. Only the overall design was specified at the tender stage, detailing was left to the successful contractor.

Rather than commissioning a test program that would provide the proof of suitability, the client decided to include the desired testing in the tender specifications, and tendered the full bridge (which involved concrete, steel and FRP) together with the FRP test program. Together with a conventional structural engineering design report, the results of the test program would be seen as a double, redundant, justification of the structure.

The winning bid for the project came from a main contractor that subcontracted all steelwork and the operating mechanism of the movable part to a steel fabricator with in-house engineering capacity. The steel contractor in turn subcontracted the design and supply of the FRP deck and its testing to an FRP Design & Build firm.

Considering the bridge as a landmark project, the successful FRP fabricator invested additionally and expanded the test program with the introduction of intentionally applied damage prior to the fatigue testing. In addition to fatigue-resistance, the tests would thus also demonstrate the absence of damage propagation that other types of FRP construction are known to be prone to.

3 Bridge design

The bridge consists of a bridge deck made of FRP with 2 steel lifting beams and 4 steel towers which contain and guide the counterweights. On the bottom of each tower an electromechanical drive unit is located. Steel cables are used to drive the movement of the bridge as well as to connect the counterweights to the bridge deck.

The steel lifting beams are shaped as a horizontal 'U', fitting around the deck and adhesively bonded (Figure 3), backed-up with vertical stainless steel pins through the steel flanges and the deck. These beams run transverse to the main span of the bridge, and include lifting points at their four ends. The connection between the deck and the steel beam was included in the test program.

The tests were executed successfully and did not result in changes to the deck design. The deck was built and inaugurated to the users in spring 2015 (Figure 4).

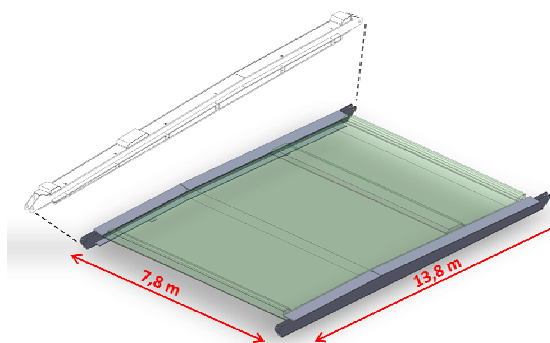


Figure 3. The design of the Pijlebrug consisting of an FRP deck spanning in between two steel lifting beams in crosswise direction.



Figure 4. The completed Pijlebrug.

4 The material FRP and its fabrication method

Fibre-reinforced polymers (FRPs) or composite materials, are combinations of load-bearing fibres and a polymer matrix. FiberCore Europe, the contracted designer and fabricator for the Pijlebrug, designs and manufactures load-bearing FRP structures using its patented InfraCore® technology. The most cost-optimal solution is to employ glass fibres in a thermoset polyester matrix. These FRPs typically combine high strength with low stiffness, compared to traditional construction materials such as steel. As such, FRP designs for bridge construction are usually stiffness-driven, resulting in low utilization ratios (unity checks typically between 0,10 and 0,20) in the ultimate limit state and a high fatigue resistance.

InfraCore® structures are sandwich-like structures where fibres in both skins also run vertically through the core, thereby eliminating the risk of skin-debonding and ensuring structural integrity at high loads and/or a high number of load cycles, even after local damage. InfraCore® panels are always built in this same manner. Depending on the application, laminate layup and panel dimensions can be varied.

5 Full-scale tests

FiberCore Europe had already conducted a constant-amplitude full-scale fatigue testing of a bridge deck. For the Pijlebrug project, additional fatigue testing at both the material level (according to methodology described in [3]) and at the full-scale level were required. The full-scale test comprised the harmonic response [4], the static deflection [5], creep during loading [6], creep during unloading [7], impact [8], fatigue [9] and ULS-loading [10].

5.1 Test setup

The inherent damage-tolerance and low utilization ratios promise high fatigue resistance for InfraCore® panels for bridge structures. To assess the fatigue resistance for bridge applications, in addition to fatigue calculations, a full-scale test specimen was produced for testing.

The test specimen measured 7,3m x 3m x 0,43m (length x width x height), which equates one lane of the bridge. Steel lifting beams were added to match the design of the full bridge. The specimen was not finished with coating or wear surface to maximize visibility of any damage or damage propagating in the test specimen. All typical construction details are included in the test coupons, so test results are generically applicable for InfraCore® structures.

The specimen was loaded at three points along the span (Figure 5), equivalent to the Eurocode fatigue load model LM4a [2], 20 million load cycles, with loads up to 200kN.

The tests were conducted at WMC (Knowledge Centre for Windturbine Materials and Construction, a cooperation between Delft University of Technology and ECN (Energy Research Centre of The Netherlands, specialized in fatigue testing of large-scale composite structures), see Figure 6. Both research facilities have broad expertise and experience in damage inspection and assessment. The fatigue test was running 24/7, and were stopped at regular intervals to inspect the specimen and assess the structure for the appearance of any new damage or propagation of the intentionally applied damage.

The full-scale tests at WMC have been witnessed by DNV-GL. While not formally required, it is common practice in the rotor blade testing

procedure to ensure compliance to the agreed testing protocol and that the tests are performed independently.

In both tests, local damage in the skin laminates of the test specimens was introduced before fatigue loading (Figure 7). In real life, such damage can occur due to collisions, accidents happening on the bridge, loose cargo falling on the bridge surface, or other causes if no crack-arrestors are in place. These local damages can potentially become a hazard to the structure if they were to grow (due to heavy loading or fatigue) and lead to progressive collapse. This is prohibited in the Eurocodes [1]. In the InfraCore® construction method, the oblique lay-up of the skins and the shear webs together prevent progression of any crack and no collapse can occur.

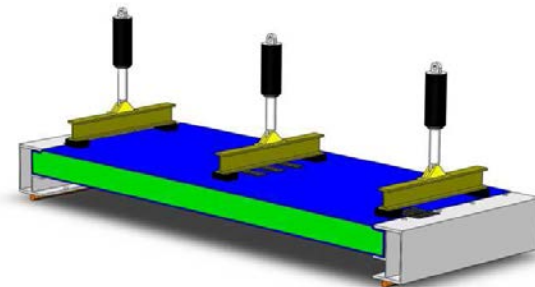


Figure 5. The design of the test setup.

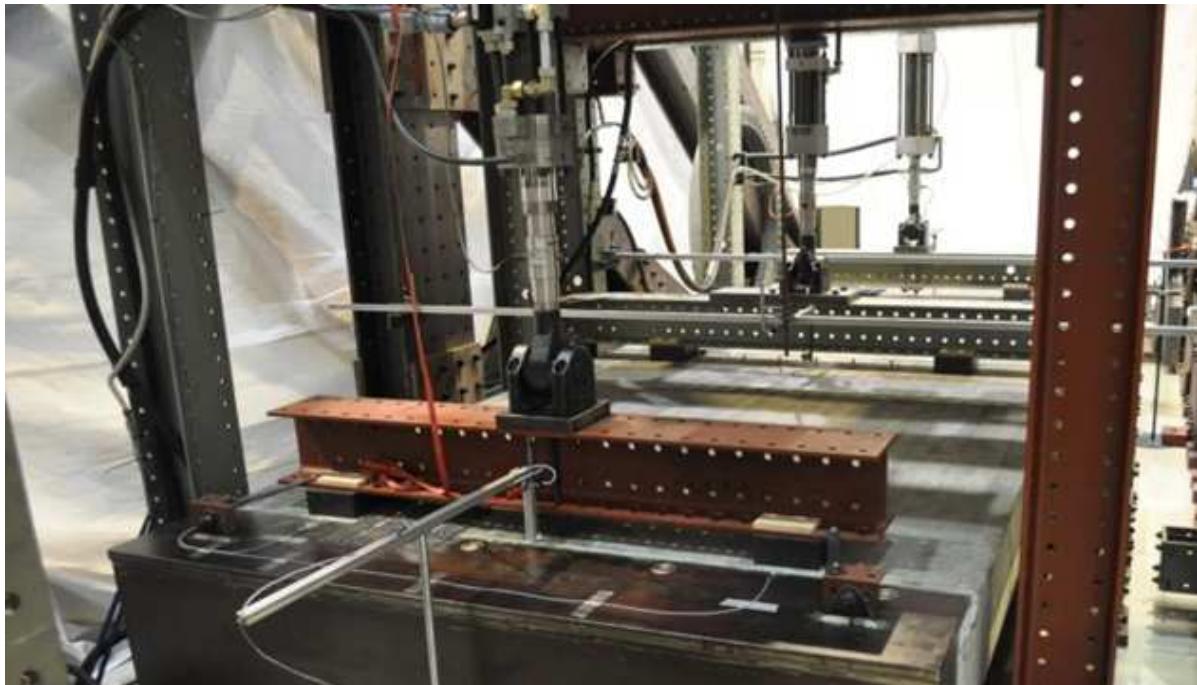


Figure 6. Full test setup at WMC. The fatigue loading is generated by three hydraulic cylinders. The load is introduced in the deck through HDPE 'wheel prints'.

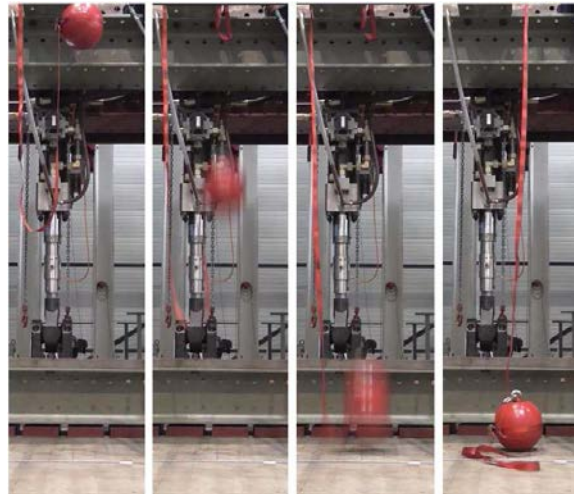


Figure 7. Impact of a steel sphere weighing 50kg, dropped from a height of 2m.

5.2 Test results

During the test and upon completion no damage initiation or damage-growth due to the fatigue loading was observed either by visual inspection (Figure 8) or infrared photography. In addition, no

decrease in stiffness was measured, showing no decrease in functionality of the structure.

After fatigue testing, the test specimen was loaded by the full Eurocode design load with partial factors included [2]. The test specimen showed no decrease in load bearing capacity.

The fatigue loading had no adverse effect on structural safety.

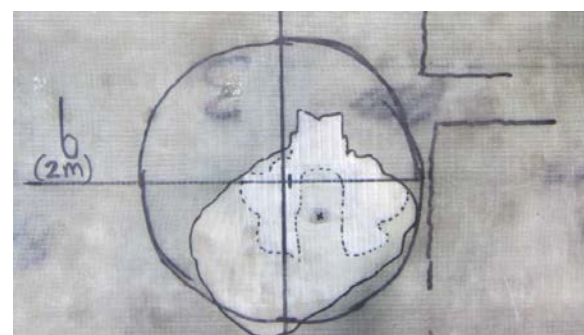


Figure 8. Local damage (delamination) in the upper skin as a result of the impact. No damage propagation was visible after the fatigue loading.

6 Material fatigue test

While full-scale tests are valuable for specific designs, results are difficult to generalise and hence do not provide evidence for all designs and load cases. The Pijlebrug deck being built using a standardised technology that is not redesigned for other applications, but only scaled, nonetheless allows for generic conclusions.

Generic use of test results requires more detailed information on material properties. For that purpose, and outside the scope of the Pijlebrug project, extensive fatigue testing on material samples have been performed to determine S-N curves in both longitudinal and transverse direction of the laminate used in InfraCore®. The test comprises a repeated cyclic load up to a certain level being applied repeatedly until failure. Higher stress levels result in a lower number of load cycles until failure.

Scientific research shows that – in contrast to e.g. steel – FRP materials have no fatigue limit and S-N curves are linear on a log-log scale [11]. Therefore, the test results can be extrapolated to higher loadings or cycle counts than such curves for metals.

The measured data in Figure 9 allows for more accurate fatigue calculations on InfraCore® structures for up to 1 billion load cycles, allowing the design of bridges intended for use in heavy-traffic areas.

Fatigue can threaten the structure at two locations in the deck; (1) at the supports in the shear webs connecting top and bottom skins and (2) at mid-span in the top and bottom skins. Using the material test results, the allowable number of load cycles can be calculated for both, taking into account the number of load bearing fibers in the principal direction.

FEM analyses and analytical approximations have shown the stress levels for the tested fatigue loading to be between 0 and 25 N/mm² at (1) (normal stress, tensile-tensile at the bottom skin, compressive-compressive at the top skin) and between 0 and 55 N/mm² at (2) (shear stress, tensile-tensile in fibre direction). As the tested fatigue loading has a variable amplitude, these maximum stresses only occur in less than 10% of the load cycles. The shear stresses in the webs are normative for the design. At the highest stress levels, the allowable number of load cycles is more than 15 million, at a confidence level of 95%.

Taking the variability of the fatigue loading into account, the allowable number of load cycles can be calculated using rain flow counting, and exceeds 100 million. The test specimen is at less than 10% of its technical life span. For excessive situations, the allowable stress can be even further increased by altering the composition or thickness of the shear webs or skins.

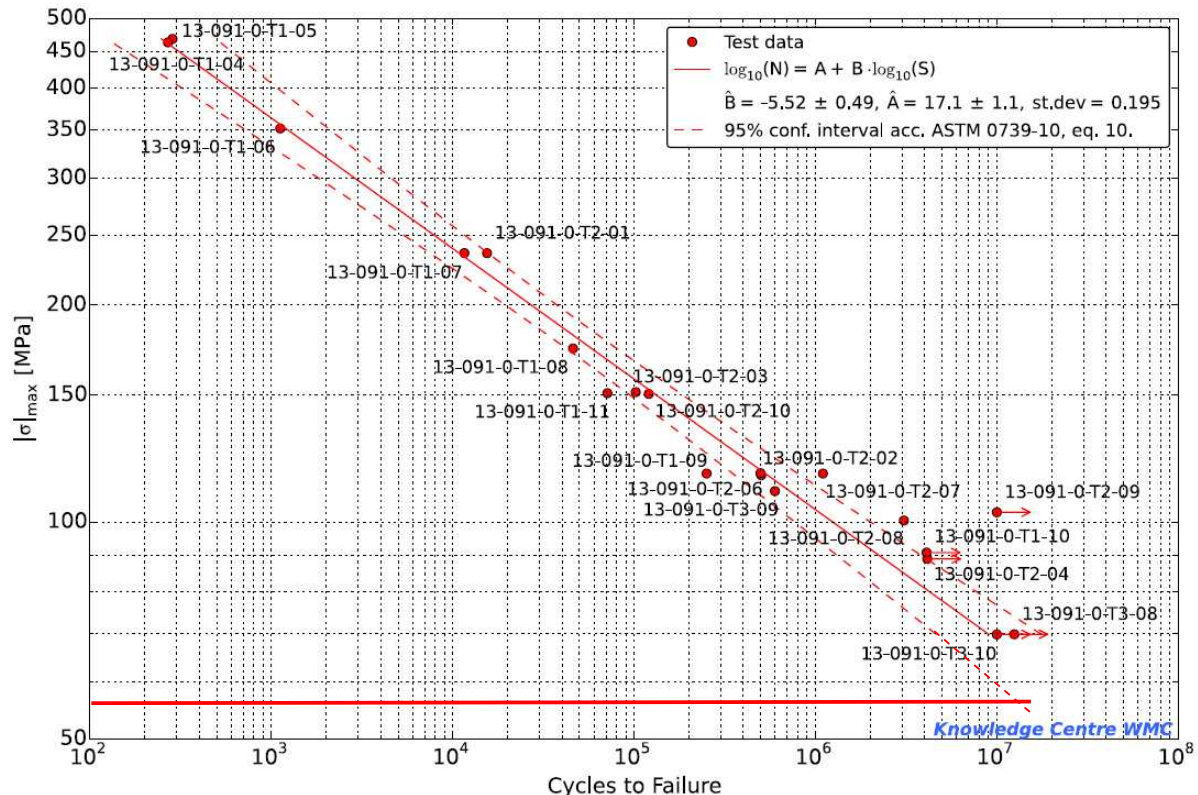


Figure 9. The S-N curve for a glass fibre reinforced polyester polymer plotted is a straight line when plotted on a log-log scale. The highest stress level occurring in the shear webs (tensile-tensile in fibre direction) is shown through the thick red line.

7 Conclusion

The client experienced the tendering of the Pijlebrug as satisfying. The successful tests increased the client's confidence in the use of FRP in civil engineering structures like bridges and lock gates.

Specifically, the client gained confidence in the engineering rules outlined in the CUR96. The testing proved the rules to meet the expectations.

In the near future the client expects FRP to be accepted as a regular construction material, like concrete or steel.

InfraCore® structural panels allow for the design of fatigue-resistant structures, such as heavily loaded bridges. The high fatigue resistance, even after initial local damage, is a result of excellent

material properties in combination with the structural cohesion of the deck's construction method. None of the full-scale test specimens have failed, the number of load cycles up to failure have yet to be determined.

The full-scale test specimen that was used suffered no damage aggravation and despite being at the end of its technical life, is expected to last much longer. Together with the fabricator owning the specimen, the client is currently looking into a new life for this structure, with the aim of monitoring it and gaining further data.

8 Acknowledgements

The authors would like to acknowledge the efforts made by all parties that were involved in this project. The required testing created an additional procedure of approval that required everyone's

co-operation over the project's duration. The project's main contractor was Macadam BV. Machinefabriek Rusthoven BV was the subcontractor for all steelwork, the operating mechanism and the movable deck.

9 References

- [1] NEN-EN 1990:2011 - *Eurocode 0: Basis of structural design*
- [2] NEN-EN 1991-2:2011 - *Eurocode 1: Actions on structures - Part 2: Traffic loads on bridges*
- [3] CUR96:2003 – Fibre reinforced polymers in civil engineering structures (in Dutch)
- [4] Knowledge Centre WMC, Pijlebrug Traffic Bridge, Test 1 – Stiffness: Harmonic response. Report number: WMC-2014-054b_2. Wieringerwerf: 2015.
- [5] Knowledge Centre WMC, Pijlebrug Traffic Bridge, Test 2 – Stiffness: Deflection. Report number: WMC-2014-054c_2. Wieringerwerf: 2015.
- [6] Knowledge Centre WMC, Pijlebrug Traffic Bridge, Test 3 – Creep: Loading. Report number: WMC-2014-054d_2. Wieringerwerf: 2015.
- [7] Knowledge Centre WMC, Pijlebrug Traffic Bridge, Test 4 – Creep: Unloading. Report number: WMC-2014-054e_2. Wieringerwerf: 2015.
- [8] Knowledge Centre WMC, Pijlebrug Traffic Bridge, Test 5 – Impact. Report number: WMC-2014-054f_1. Wieringerwerf: 2015.
- [9] Knowledge Centre WMC, Pijlebrug Traffic Bridge, Test 6 – Fatigue. Report number: WMC-2014-054g_2. Wieringerwerf: 2015.
- [10] Knowledge Centre WMC, Pijlebrug Traffic Bridge, Test 7 – ULS test. Report number: WMC-2014-054h_2. Wieringerwerf: 2015.
- [11] ASTM E739 - Standard Practice for Statistical Analysis of Linear or Linearized Stress-Life (S-N) and Strain-Life (ϵ -N) Fatigue Data



New concepts in movable lightweight bridges in fibre reinforced polymers (FRP)

Martijn Veltkamp, Arnoud Haffmans

FiberCore Europe, Rotterdam, the Netherlands

Contact: veltkamp@fibercore-europe.com

Abstract

Low maintenance and low self-weight are two of the most important advantages of using fibre reinforced polymers (FRP) as structural material for bridges in general, and movable bridges in particular. These advantages count in both new-built and refurbishment projects. In the last few years, a variety of such structures has been constructed, enabling to compare the different typologies, their experiences and an outlook on how FRP can best be used to further employ its full potential.

Keywords: Fibre reinforced polymers (FRP); movable bridges; structural topology; lightweight.

1 Introduction

Explicit consideration of life cycle costs at early project-stages has made clear the need for more durable, less maintenance-intensive structural materials. In parallel to the required design-life becoming longer, a maintenance-regime needs to be in place to realise this ambition. The FRP-material being durable and not being prone to degradation to known aggressors such as water, salts and UV-radiation, eliminates a large part of the structurally necessary maintenance-intervals needed for conventional construction materials.

In movable structures a low self-weight presents a range of indirect advantages in addition to the reduced permanent loading only. For design, it results in more slender bridge spans with less voluminous counterweights. In the construction stage it implies a shorter building time due to a lower mass of the prefabricated parts. In use, a lower mass has less inertia and requires less energy to move, lift or rotate.

Other than in new-built, FRP also enables retrofitting and upgrading of existing structures. The ageing stock of existing infrastructure includes structures that no longer meet the design loading requirements and performance criteria that have gradually been upgraded over time. While structures may have been built with some intentional redundancy in them, or with a hidden capacity that can be demonstrated through modern means of assessment, both are rarely the case for the bridge deck. The deck is often built in steel or timber and suffering most from degradation under the influence of water, de-icing salts or fatigue.

Dependent on the type of fabrication, the FRP material is resistant to both impacts and de-icing salts and replacing the bridge deck implies an upgrade in both quality and capacity. For refurbishment projects the challenge generally is to provide upgraded load-bearing capacity, possibly including a widening, within the same nett weight as the original structure in steel. This

way parts of the existing structure can be maintained, resulting in significant savings in time, hindrance and cost. The deck representing a large portion of the structure's self-weight, weight-savings on the deck therefore also result in significant overall weight-savings.

2 FRP in civil engineering

Glass fibre reinforced polymers, GFRP, combine high strength with low stiffness when compared to steel, the conventional structural material used in moveable bridges. Using these characteristics in a material-specific design will create the best structure, with a high value to the owner. Such design-for-stiffness look and behave different to conventional design-for-strength structures, and are also safer and more future-proof.

2.1 Strengths and weaknesses of FRP

Using the infusion-technique for the fabrication of FRP structure gives ultimate freedom to define shapes and structural properties. Prior to infusion, the glass fibre fabrics can easily be formed to the structurally efficient typology of skins with webs in between, like rolled steel profiles. A foam core acts as lost mould until infusion with resin, once cured resulting in an on average lightweight panel.

Combining a high load-bearing capacity with a low self-weight, makes the FRP material a promising candidate for the use in movable bridges. However FRP is an umbrella-term for all sorts of resins, fibres and fabrication types.

In civil engineering, for economic reasons FRP is typically based on glass fibres in a polyester matrix. The stiffness of GFRP being about $1/5^{\text{th}}$ of steel ($39 \cdot 10^3$ vs $210 \cdot 10^3$ N/mm 2 , combined with fabrication limits on the skin-thickness, makes that designing in FRP requires activation of sufficient width to stay within deflection limits typical for road bridges. Spans are therefore best realised as slabs, rather than beam-and-girder arrangements. As will be demonstrated later, this also introduces alternative load paths, contributing greatly to achieve a robust structure.

The design being driven by stiffness, results in low stresses, making FRP particularly resistant against

fatigue. This lengthens the design life and results in safer structures.

Other than FRP's specific strength and stiffness, also to be considered is its time-dependent behaviour. Like concrete, FRP shows a creep effect in case of long-term loading. Since the creep effect is due to the cured resin matrix, a higher fibre content in a certain direction not only results in a higher stiffness, but also a reduced creep effect. Creep brings the favourable aspect that the bridge will deform to its bearings, bridging any imperfections and reducing noise when loaded-unloaded.

2.2 Requirements on FRP used as decks for road bridges

To be also suitable as the deck driven on by the overall traffic, the deck should not only be sufficiently strong and stiff for the specified loading. It should also be resistant to impacts and be robust in accidental situations, over its full design life. This requires that there should be no progressive collapse and that there is a warning mechanism rather than a sudden failure.

In general, progressive collapse can occur when structures feature little coherence and operate at high utilization ratios. A local failure of the structure due to an accidental load should not worsen to an overall failure. Secondary load paths should be capable of taking over the load transfer. However if that is highly loaded already, also the secondary load path fails.

In FRP decks built as a large single component with the infusion method, the fibre and fabric arrangement is highly multi-axial, and acts as a two-way spanning system. Primary and secondary load paths are thus present in the same structure, and no matter where the accidental failure occurs, the load path can always be deviated. Low utilization ratios in terms of strength, allow for overloading without failure. If an overload leads to local damage, repair is not urgent while multiple load paths redistribute the loading.

The structure should also be resistant against unforeseen loads and loads in unforeseen directions. To achieve this, nowhere in the structure therefore the portion of fibres in one

direction exceeds 80%, this way always keeping sufficient strength in the transverse direction.

Unique to the InfraCore® construction type is that along the full span the structural integrity does not rely on any bonded areas between fabric layers. Even if this would be totally absent, the deck retains its structural capacity since fibre-reinforcement runs continuously from the top skin, via the shear webs, to the bottom skin. Deck-compositions consisting of skins and shear webs that are bonded together do not have such integrity, have no crack-stopping properties in case of delamination and therefore still pose a risk (Figure 1), and are not acceptable.

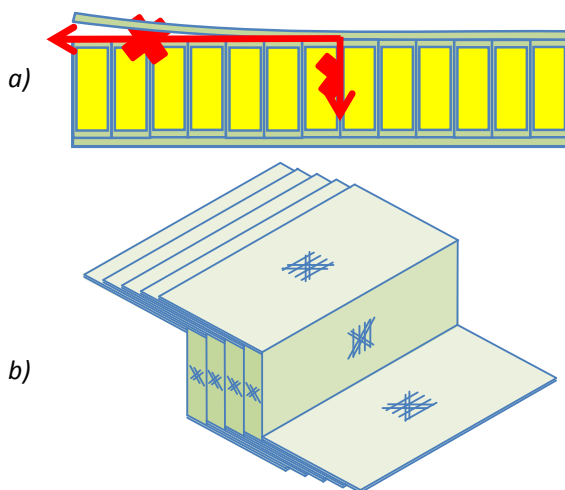


Figure 1. Robustness of FRP road decks: a) Sandwich-like build-ups risks overall failure in case of delamination and are therefore unsafe. In b) instead, continuous fibres from top skin to bottom skin may delaminate without consequence.

The warning mechanism in case of imminent failure is inherently part of the low utilization ratio of FRP structures. With residual load bearing capacity available, the deflection will increase with increasing load in a fully elastic manner. Overall strength utilization in the ultimate limit state could be as low as 20%. Using this over-capacity, the 5 times (reversible!) over-deflection acts as a warning signal.

2.3 Application areas for FRP in movable bridges

Considering its properties, for FRP the most suitable structural types are self-supporting,

integral, sandwich-like structures of medium span, subjected to high loads in a large number of load-cycles. For the introduction of local high loads, such as at hinges and suspension points, metal elements can be used, either as inserts or as external steel elements.

3 Movable bridges with infused FRP decks

Movable bridges exist in various typologies that over history have been realized in different materials. To this stock of precedents, over the past few years nearly all typologies have also been realized in FRP. The list hereafter sums up how FRP has been incorporated in the typologies, show their realization as a bridge, and suggests design-directions to exploit its potentials further.

3.1 Drawbridge

The most traditional of the movable bridges is the drawbridge (Figure 2). In closed position, the deck spans as a self-supporting element between the abutments. When opened, the tension guys lift the deck aided by the counterweight attached to the other end of the lever arm. The force needed to operate is only to overcome the slight imbalance. FRP being used as structural material for the deck results in a lighter deck, and thus requires a lighter counterweight, in turn reducing the weight of the superstructure. This gives a more slender design.

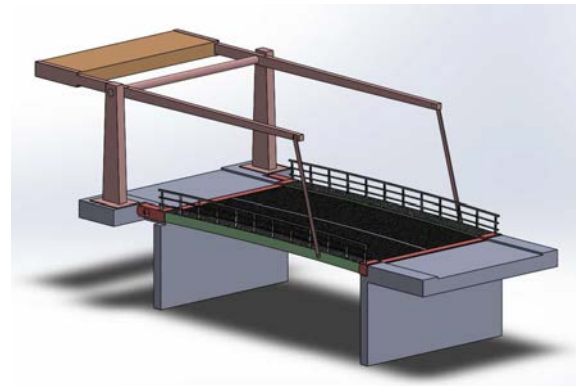


Figure 2. The principle of a drawbridge.

The hinges are typically realized in steel and no FRP alternative yet exists due to the required high local stiffness. To transfer the forces from the

bridge to the hinge, a steel beam is therefore needed, acting as the support for the deck, yet being rigidly connected to it to transfer a limited bending moment close to the support.

Point of attention of this bridge type is the permanent exertion of the upward forces from the counterweight at the points of attachment of the tension guys, and any downward forces applied by the spindle. Combining load-reduction through a lightweight deck, spreading the load through steel inserts and local adaptation of the FRP-laminate keeps the expected and predictable creep effect within acceptable limits.



Figure 3. The refurbished Elburgerbrug (NL), with an FRP deck.

Figure 3 shows the 12m clear span Elburgerbrug (Netherlands). In 2015 the bridge was refurbished, which included replacing the fatigue-damaged

steel deck by an FRP deck of higher load-bearing capacity within the same weight (60.000kg). This upgrade was to meet Eurocode load models 1 and 2, as opposed to the lower design loading of the design standards used when the bridge was built in 1956. This way the superstructure and the operating system could be retained, contributing to the economy of the project. A full-steel deck would have weighed 25% more and required replacement of the superstructure.

Due to the change from beam-and-girder arrangement to that of a plate-deck, the structural depth was reduced from 1000 to 700mm, and the clear height for passing ships increased. The hinges were renewed yet located at the same position. At the opposite end, the deck was supported on the existing abutments, which required introduction of a steel end beam at the tip. The beam in itself is supported at two points, yet acts as a linear support for the FRP deck.

The materialisation in FRP combined with steel of this typology can be further optimised, as is shown in Figure 4. For new-built bridges, the abutment would be designed to act as linear support for the deck, thus removing the need, weight and complexity of a steel beam at the tip. Encapsulating the steel beam and the hinges in FRP would be a further improvement to reduce stress concentrations and minimise the amount of steelwork exposed to the environment.

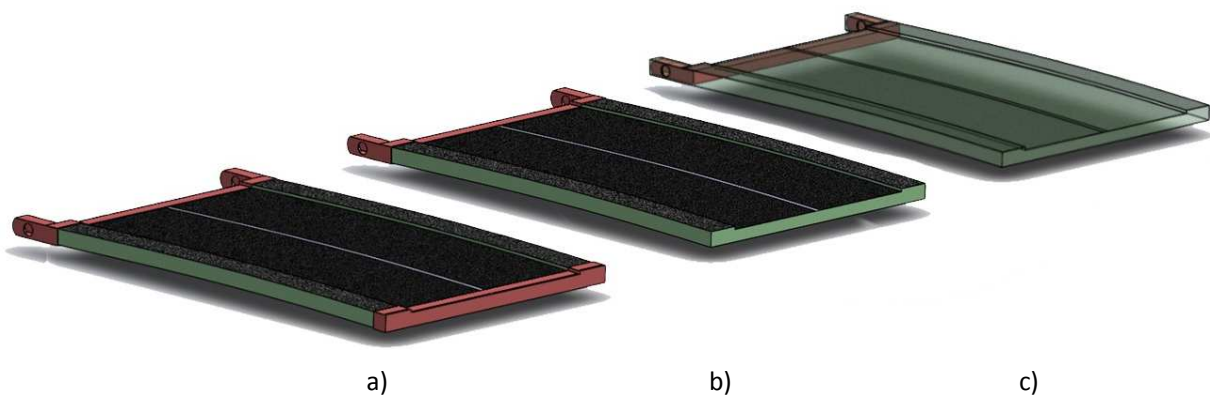


Figure 4. Three stages of FRP-steel hybrid bridge decks: a) steel end-beams at both ends in refurb situations; b) with only a steel beam at the back-end in new-builds; c) with encapsulated steelwork.

3.2 Bascule bridge

In a bascule bridge the counterweight is directly connected to the deck, typically below it (Figure 5). This eliminates the need for a structure above deck level, and enables wider bridges without intermediate obstacles. The counterweight is the main disadvantage of this typology, due to its size and place. When placed below the deck its housing needs to be waterproof, requiring extensive foundations in situations where the deck is low above the water. Positioned above the deck it gives a limitation to the clearance for the traffic.

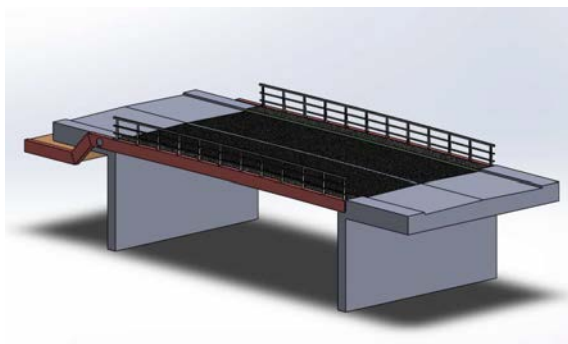


Figure 5. The principle of a bascule bridge.

Reducing the self-weight of the deck alleviates the burden of the counterweight. This is a well-known challenge and to do this decks have been equipped with timber or aluminium planking, or realized in aluminium altogether. Longevity of both is limited, especially due to ever increasing axle loading, traffic densities and availability requirements.

The counterweight generates a permanent bending moment at the position of the hinges. These localised forces are difficult to introduce in FRP only, and hence a hybrid with steel is desirable here.

An FRP deck in between two longitudinal steel side-beams overcomes this: in closed position the deck acts as a self-supporting element between the abutments. Steel is used for the hinges and the back span. To connect the FRP deck to the hinges, a longitudinal steel beam is proposed. Although running in the deck's span-direction, the beam only carries the deck when the bridge is opened, and the deck spans in transverse

direction. The transverse span may well be longer than the primary span since there is no traffic loading in this situation.



Figure 6. The Spieringbrug near Muiden (NL) has no counterweight and is operated through the cylinders only.

The extreme case of a lightweight deck has been realized in the Spieringbrug near the historical town of Muiden, the Netherlands (Figure 6). The bridge carries two lanes for traffic and a bicycle path. Here, the deck was of such low self-weight that no counterweight was required. The bridge opens through sufficient force generated by two hydraulic cylinders. The cylinders connect to the longitudinal beam that was rigidly connected to the deck using the same connection principle as applied before along the full 142m length of the FRP-steel hybrid truss-bridge across the A27 motorway near Utrecht, the Netherlands [1].

As a refurbishment project, the deck of the Klaffbron in Malmö (Sweden), see Figure 7, will be equipped with an InfraCore® FRP deck replacing earlier aluminium and timber decks. Within the same structural depth (115mm) as the existing deck, the new deck will have the same weight (100kg/m^2) and thus require minimal changes to the counterweight, yet features a higher load-bearing capacity and a longer design-life than its predecessors.



Figure 7. The Klaffbron in Malmö (SE) will be refurbished with an FRP deck replacing the earlier aluminium and timber decks.

3.3 ‘Swing chair’ bridge

Building on from the advantageous use of a lightweight deck in the bascule bridge, a new concept was developed. Of similar typology to the bascule bridge, but materialized as a continuous FRP plate: a bridge-deck at one end, to a hollow panel containing the counterweight at the other end. This concept employs the flexibility of FRP construction, that can be moulded at relatively low cost.

Steel is used for the operating mechanism, at the hinges and the cross-beam below the deck. To achieve sufficient clearance to open, the axis of rotation is at the deck-level, thus giving the steel beam the shape of a swing chair (Figure 8). This concept has a minimum quantity of steel exposed to the exterior environment, this way minimizing maintenance and extending the life expectancy. Its hinges are accessible for maintenance and replacement when needed.

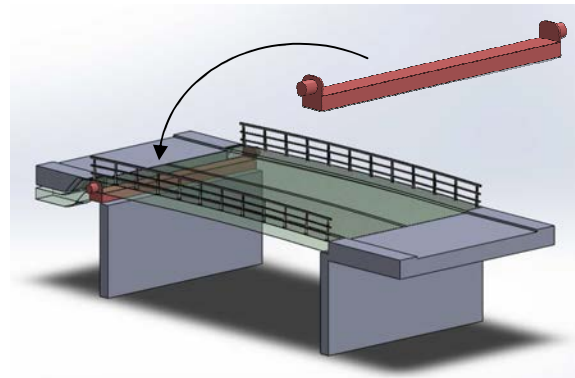


Figure 8. The principle of the swing chair bridge, with the swing-chair steel beam shown separately.

3.4 Swing bridge

The swing bridge rotates around a vertical axis, and is sometimes raised before rotation. In open position, the deck of a swing bridge cantilevers from the pivoting point, while in closed position the deck rests on both ends as well as the pivot (Figure 9). The pivot being relatively small compared to the width of the bridge, an additional structure in steel is necessary to provide a bearing over the full width of the deck.

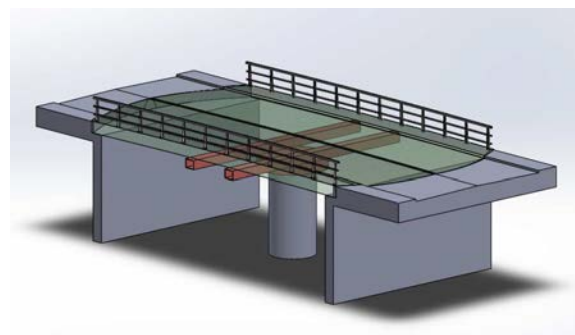


Figure 9. The principle of a swing bridge.

A lighter deck requires less structural depth in its substructure and results in a further reduced self-weight, in turn resulting in a lower moment of inertia and faster operation with a lower power engine. Further savings of FRP decking could be achieved in shorter approach spans, or the potential for a wider clearance for passing ships, or an asymmetrically placed pivot point.

For the 6m width, 48m main span swing bridge in Souburg (the Netherlands) and its 17m approach span (Figure 10), an infused FRP deck was the client’s preferred refurbishment solution. Key

drivers were the deck's water-tightness, low maintenance and low self-weight. The low self-weight allowed for widening the bridge by 1m with a walkway on the outside of the truss. Even with this addition, the mass of the swing-part was reduced from 165.000 to 140.000kg.



Figure 10. The heritage Souburg (NL) swing bridge, refurbished and widened with FRP decks.

The bridge structure, originally from 1907, the approach span from 1870, comprises primary trusses, symmetrically cantilevering from the pivot, with secondary beams in between and timber planking deck on top. The original deck, despite its asphalt finishing, was not watertight and water ingress had caused substantial damage in zones of difficult access. The new deck was to be watertight, and therefore produced as large prefabricated elements, and arranging the water runoff to end of the bridge rather than through the deck. To close the gaps left by the diagonals running through the deck, custom-cut plates with a small upstand were placed on top of the deck and a minimum of water will come through this.

3.5 Lifting bridge

In a lifting bridge the deck is moved in vertical direction (Figure 11). The lifting cables are connected to the corners of the deck. At the other end, the cables connect to counterweights and an engine powering the movement. A lower mass to be moved naturally results in a more energy-efficient operation, and in a more slender superstructure.

Replacing an earlier bridge, the province of Drenthe desired the new Pijlebrug road bridge across a canal near Meppel (the Netherlands) to have an FRP deck. The tender documents showed

the outline of the bridge, which was to have steel lifting beams at both ends, extending beyond the deck where the lifting points are attached. The connection of the FRP deck to the lifting beam was by slotting it into a horizontal U-shape, which was then bonded and mechanically secured. In closed position, the lifting beam is resting on pot bearings that are just offset from the transition from FRP to steel.

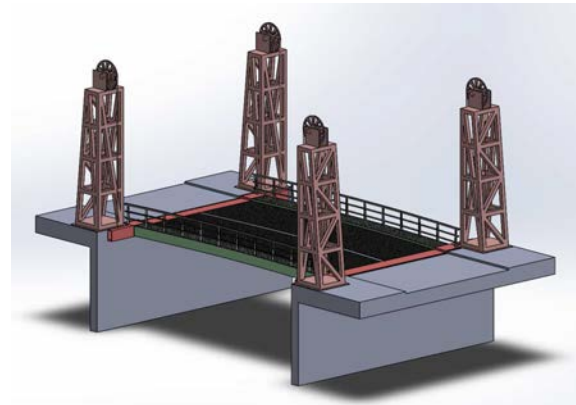


Figure 11. The principle of a lifting bridge.



Figure 12. Construction of the new Pijlebrug lifting bridge, with an FRP deck.

The client was familiar with FRP through a set of lock gates it had commissioned a few years before. To demonstrate the fitness of the material, the client required both conventional engineering calculations, as well as a full-scale test on a full-span sample equivalent to the eventual bridge, with a width of one lane. The structure was loaded by fatigue, following intentional initial damage, and tested to withstand full ULS loading at the end. All tests were passed and confirmed the structural design. Design, testing and its

conclusions are described in [2]. The bridge was opened to traffic in spring 2015 (Figure 12).

3.6 Table bridge

Moving in vertical direction like the lifting bridge, the operating mechanism of the table bridge is located below the deck (Figure 13). The visual obstruction of a table bridge is therefore limited, unlike the lifting bridge that requires a fixed structure that is always higher than the movable part. The vertical push-up requires specific attention to the stability in the raised position.

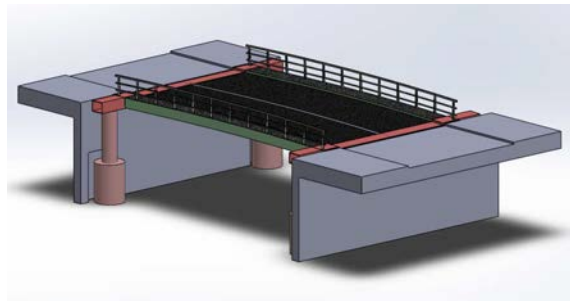


Figure 13. The principle of a table bridge.

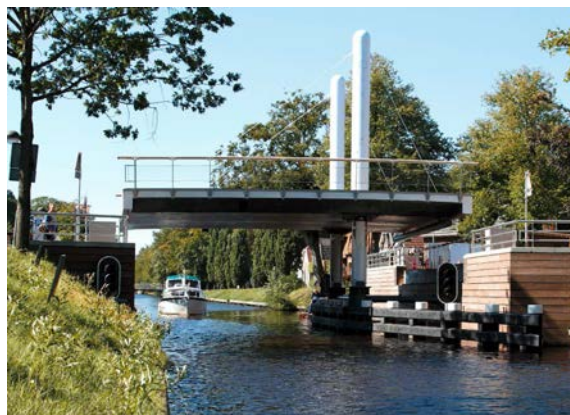


Figure 14. The Oosterwolde table bridge with its eccentric lifting point (picture by Martin Reidsma).

For a new movable road bridge to be built in the inner city of Oosterwolde, the Netherlands, the client organized a design competition that was won by a consortium of an architect and an engineering consultancy. The design entailed an operation mechanism of only two cylinders placed in the water (Figure 14). This kept the abutments free from any additional structures, however to provide sufficient clearance width for ships to pass, it required asymmetrical supports. FRP was the solution to achieve a low self-weight deck in

order to keep the structural dimensions and operating mechanism small. In addition, the voids inside the deck were filled with (invisible) lead blocks to balance the deck. The bridge is in use since 2010.

3.7 Further typologies of movable bridges

This list of movable bridge typologies cannot be exhaustive. By combining the ingenuity of mechanical engineers with the structural engineer's understanding of FRP's characteristics and degrees of freedom, including the results of ongoing developments on the materials-side, further concepts can be developed.

4 Conclusions

While building in FRP is not yet commonplace and its acceptance shows wide variations across the world, it represents significant advantages of low-maintenance and a long design life. Also its higher safety and capacity for future load-increase are of interest to the client and the public. The further advantage of a low self-weight makes it an advantageous material for constructing decks of movable bridges for road usage. A variety of typologies and their realisations was presented and hints at further realisations to come.

5 Acknowledgements

Designing and constructing bridges is teamwork, and even more so for movable bridges in FRP that include steel parts. While shown from the perspective of the FRP-material for the purpose of this paper, the shown realisations could not have been achieved without the contribution and willingness of any member of the client and the team involved.

6 References

- [1] Veltkamp M., and Peeters J. Hybrid Bridge Structure Composed of Fibre Reinforced Polymers and Steel. *Structural Engineering International*. 2014; 3: 425-427.
- [2] Hiddingh J., Grefhorst R., and Veltkamp M. *Full-scale fatigue testing with initial damage as validation of FRP road bridge design*. IABSE conference 2016, Stockholm (forthcoming).



Monitoring and Inspection of a Fiber Reinforced Polymer (FRP) Road Bridge

Markus Gabler

Arup, Dusseldorf, Germany

formerly: Institute for Building Structures and Structural Design (ITKE), U. o. Stuttgart, Germany

Eberhard Pelke

Hessen Mobil, Wiesbaden, Germany

Jan Knippers

Institute for Building Structures and Structural Design (ITKE), University of Stuttgart, Germany

Contact: markus.gabler@arup.com

Abstract

The Friedberg Bridge in Germany was the first FRP - steel composite road bridge in Europe when it was opened to traffic in 2008. The bridge has a span of 27 m and a total width of 5 m. It had been designed for full vehicle live load as per EN 1991 with the then applicable NA for Germany. An extensive sensor network had been installed to investigate the structural behavior of the bridge when subjected to daily temperature cycles and live loads. The bridge has also been visually inspected over the first years of use.

This contribution will present the sensor readings during load tests and daily temperature cycles. The results allow for assessment of the load bearing behavior of the FRP deck and adhesive interface of the deck to the steel girders as well as long-term effects. This can be used for calibration of a detailed FEA model of the bridge, which can be used for future design tasks of FRP bridges. For example, the analysis shows that the contribution of the surfacing layer as well as the parapets is non-negligible for proper modeling of the structural behavior.

The load testing was supplemented by visual inspections, which didn't showed any visible damage to the adhesive layer nor the FRP deck.

Keywords: FRP; GFRP; Monitoring; Sensors; SHM; Adhesive; Maintenance

1 The Friedberg Bridge

1.1 Structural System

The Friedberg Bridge has a steel – FRP composite superstructure. Both components are adhesively bonded together with an epoxy grout (Figure 1). The superstructure is fixed to both RC abutments and thus forms a frame structure. The advantage is that hogging and sagging moment are of similar

magnitude. Compared to a simply supported beam, this allows for a slender design. Also, a central pier can be omitted. The composite action achieved by the FRP deck reduces the vertical displacement of the superstructure by approx. 20% compared to the steel girders alone. This is less than with steel – concrete composites, but still a significant saving.

The design of the bridge and laboratory testing had been shown in previous publications [1][2] [3].

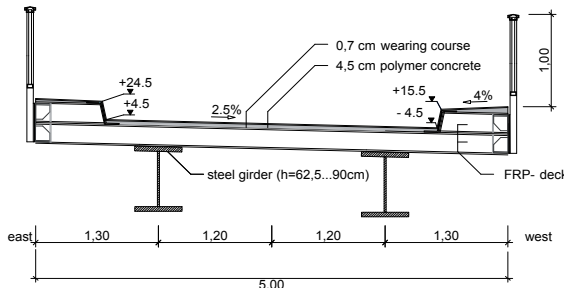


Figure 1: Composite cross section of the Friedberg bridge with steel girders and pultruded FRP deck

1.2 FRP deck

The FRP deck is built out of pultruded hollow sections (FDB 600 "ASSET" from Fiberline Composites, Denmark). Pultrusion is a process where continuous fibers are pulled through a heated die with liquid resin (e.g.: unsaturated polyester) in a fully automatic process. Pultruded profiles show excellent mechanical and geometrical properties with little deviations and are the most economic competitive solution [4]. After production, the prismatic units are cut to necessary lengths and subsequently adhesively bonded together to achieve an aerial slab. Other connection techniques such as bolted or snap-fit joints [5] serve only to fix the bars but don't provide full load transfer within the deck. These techniques are thus not recommended for bridge design.

Finally, the deck is adhesively bonded to the steel girders. As opposed to bolted connections, bonding allows for a smooth load transfer and does not weaken the FRP material. Steel – FRP composite is a very economical solution since the steel girders contribute the overall load bearing capacity but are well protected against weather and de-icing salts, while the FRP deck only needs to contribute local load transfer and shows excellent corrosion resistance.

The wearing surface is a crucial component of FRP road bridges since it has to provide a rough and durable surface as well as re-distribution of concentrated wheel loads. Among different materials, polymer concrete shows optimal adhesion to the FRP deck as well as best performance during temperature changes and abrasion [6]. Polymer concrete is a mixture of 50% to 90 % by wt. silica and epoxy resin. It proved essential to adjust the aggregate size to the layer thickness.

1.3 Detailed FEA analysis

In order to better understand the load bearing behavior of the superstructure, a detailed FEA model has been generated. Opposed to common structural systems for bridges, the parapets and the surfacing layer have been taken into account in order to obtain results which are as realistic as possible (Figure 2). The used material properties are average values which have been mostly been gained from pre-production tests (Table 1).

Table 1: Material properties used for the FEA model

	moduli of elasticity [N/mm ²]			Poisson ν_{yx}	strength [N/mm ²]		thickn. [mm] t	
	E_x	E_y	G_{xy}		$f_{x,u,k}$	$f_{y,u,k}$		
GFRP deck	flange	28,000	19,000	5,000	0,3	250	175	15,6
	glued web	17,000	24,000	4,500	0,2	165	125	10,0
	inner web	17,000	26,000	3,000	0,2	210	200	14,0
	E	$f_{t,u,k}$ (*)	$f_{s,u,k}$ (*)	thickn. [mm]				
surfacing layer	25,000	2,3	4,3	45				
adhesive layer	8,000	1,1	8,8	7				

x: direction of pultrusion, here: perpendicular to bridge
y: perpendicular to direction of pultrusion, here: along bridge
t: tension
s: shear
(*) in conjunction with the flange of the GFRP deck

While it was possible to determine the properties of steel, FRP and adhesive with little uncertainties, it proved more complex to estimate the stiffness of the substructure and foundations. The stiffness is also subjected to change during the bridge's service life: it is known for backfilled frame structures that the horizontal stiffness is consecutively decreasing over time due to compaction of soil behind the concrete wall.

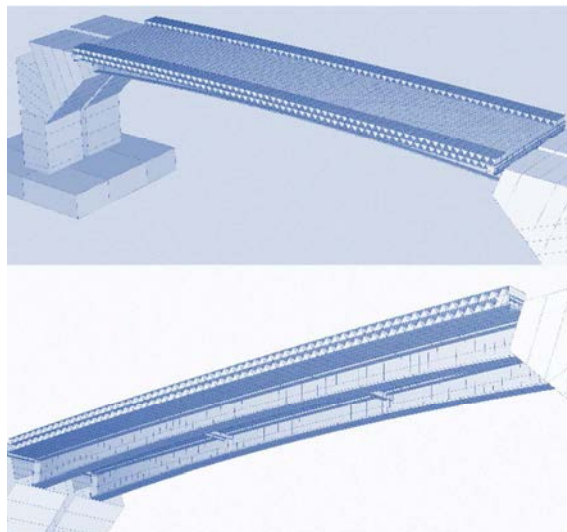


Figure 2: FEA model of the Friedberg Bridge

1.4 Construction

The superstructure had been completely prefabricated in a workshop, which included deck, adhesive layer, parapets, surfacing layer and railings. During assembly, various strain gauges, fiber optic sensors (FOS) and temperature sensors have been applied on the structural components and within the surfacing layer. These sensors would later be used for the monitoring. After the superstructure had been finished, it was hauled to the construction site and lifted in place within only two hours. Due to the low dead load of the superstructure (~60 tons), the transportation and lifting could be performed with standard construction site equipment (Figure 3).

The superstructure was placed into pockets of the RC abutments which had been grouted to achieve the structural system of a frame. This means that the dead load moment curve is as with a simply supported beam and only live loads will act on the frame structure.



Figure 3: Superstructure erection in July 2008

2 Monitoring Program

2.1 Sensor setup

The sensor network on the bridge serves scientific investigations as well as to check reliability of the adhesive layer between steel girders and FRP deck. In total, 95 electronic strain gauges have been applied on the surfaces of the GFRP deck and the steel girders. The strain gauges are thin film resistor strain gauges (*HBM series Y, quarter bridge coupling*), which have been chosen according to the coefficient of thermal expansion of the particular substrate. 12 of these strain gauges had been later embedded into the adhesive layer.

On the identical positions, 12 additional fiber optic sensors have been placed on the surfaces in order to secure redundancy of these sensor locations at the most important structural detail of the superstructure. These fiber optic sensors work with Fiber Bragg grating (*FIBERSENSING CFRP layer*). These sensors work via modulation of light wavelength which is guided through an optical fiber, the strain at the measurement point can be derived from the measured wavelength shift. Fiber optic sensors are known to have a much longer service life than electronic strain gauges and therefore mainly serve for checking of the adhesive layer.

Also, 6 temperature sensors have been placed in or on the superstructure to measure temperature shifts and temperature gradient (*OMEGA type T*).

The sensor are numbered and placed according to the overall load effects they should help to analyze (Figure 4, Figure 4 /Figure 5):

- Load case 1 (series 100): strain sensors on bottom surface of the FRP deck, orientation alongside bridge span, purpose: investigation of effective width of FRP deck as part of main load bearing structure (composite action)
- Load case 2 (series 200): strain sensors on bottom surface of GFRP deck, orientation perpendicular to bridge span, purpose: investigation of load distribution of concentrated wheel loads within FRP deck spanning between steel girders

- Load case 4 (series 400): strain sensors on each height of the cross section, orientation alongside bridge span, purpose: investigation of strain distribution over the cross section, verification of Bernoulli strain distribution
- Load case T (series 500 and 400): temperature sensors on each height of the cross section, combined with strain sensors, purpose: investigation of restraint stresses in the superstructure when subjected to temperature shift.

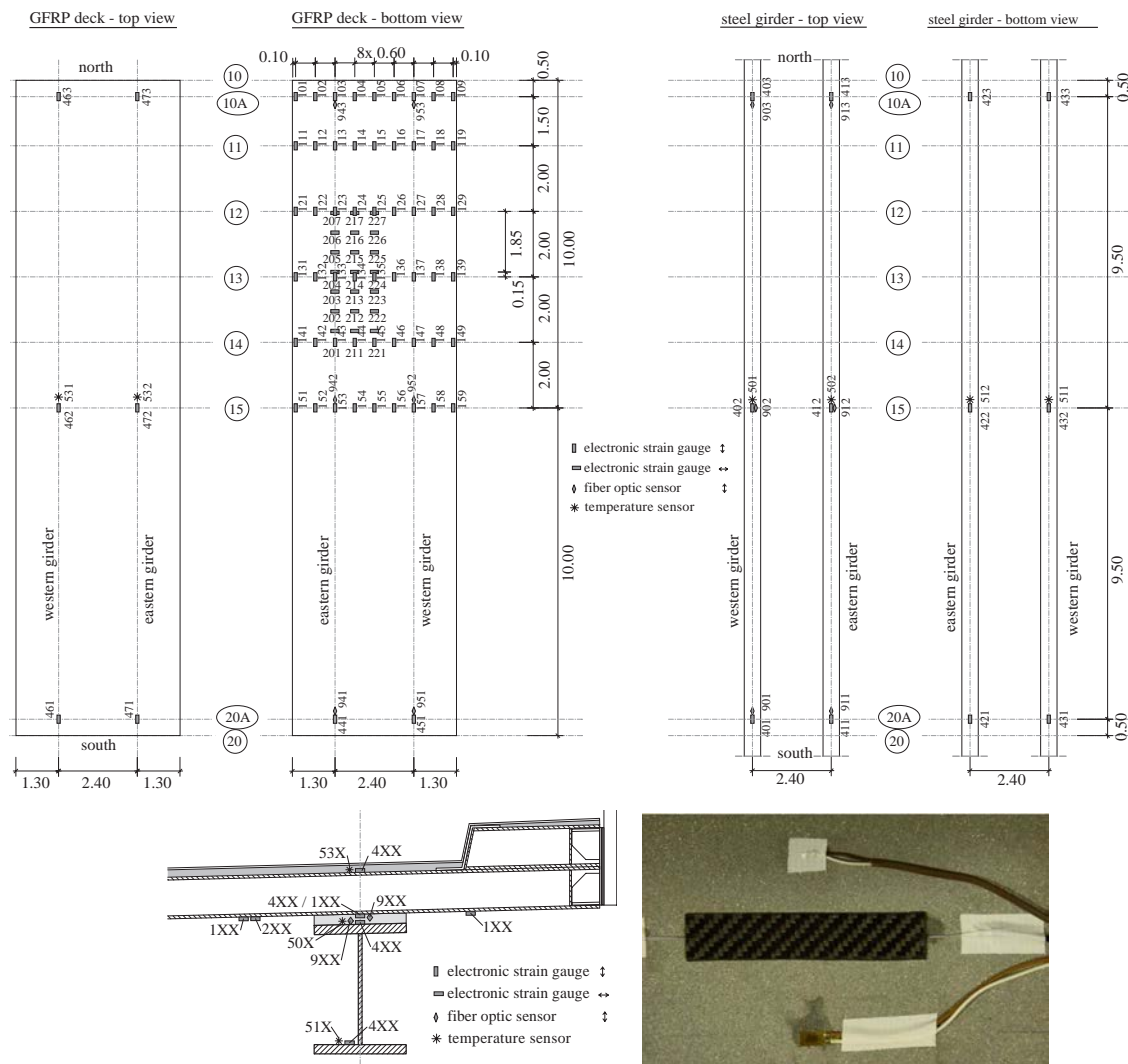


Figure 4 /Figure 5: Sensor locations

2.2 Load position and values

Due to the sensor layout, two different load positions were investigated. For load case 1, the rear axle of the truck is placed 11 m from the northern abutment (Figure 6). Thus, the strain in the sensors placed between gridline 10A and 15 will be subjected to a mainly uniform strain

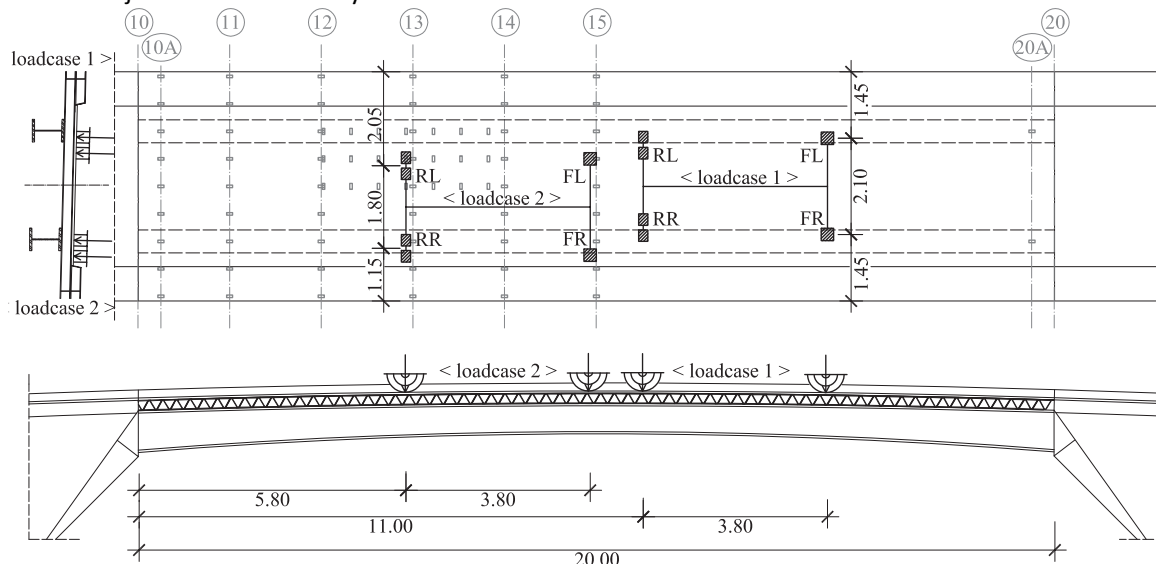


Figure 6: Investigated load cases; Load case 1 for global bending, Load case 2 for concentrated wheel loads

The use of a loaded truck for the tests resulted in a variation of the absolute load as well as the distribution within the wheels. While the measurement results can be scaled to a uniform absolute load (i.e. 200 kN), the variation of the distribution leads to significant uncertainties. The FEA model is analyzed with each load distribution to evaluate the effect of non-uniform distribution.

The other variants are the temperature within the superstructure as well as a possible shift in the structural system due to time dependent effects such as creeping or change of stiffness of the backfill.

2.3 Measurement

The strain distribution is mainly gathered by electronic strain gauges. As mentioned above, for every strain gauge within the adhesive layer, an additional fiber optic is being placed in order to double check results and to provide more reliable sensors for this critical structural detail.

distribution. A truck position in the very center of the superstructure would lead to higher bending moments but disturb the strain distribution in an undesired way. For load case 2, the rear axle is placed at the centre of the load case specific sensor array, which is close to gridline 13 (also Figure 6).

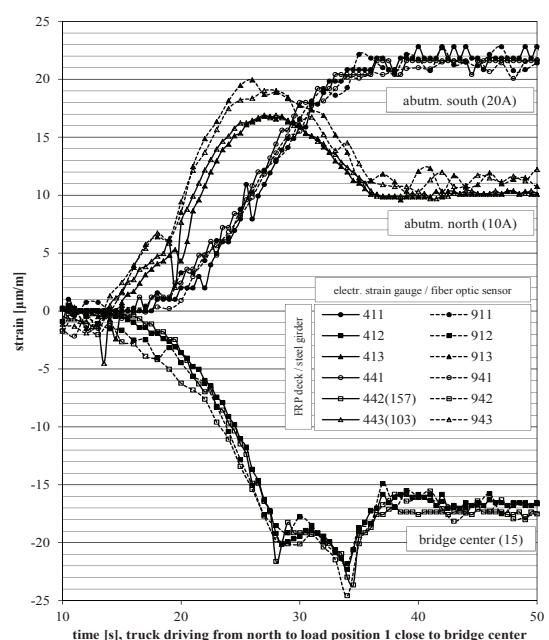


Figure 7: Measurement during truck load test,

The strain record shows that both sensor types yield to identical results for the adhesive layer (Figure 7). The graph compares the results from electronic strain gauges (continuous line) to that of fiber optic sensors (dashed line). The results of the two abutments are different since the truck is not exactly located in the center of the bridge. The filled markers denote the strain at the steel side of the adhesive layer and the void markers the strain at the FRP side of the adhesive layer.

Since the steel girder of the superstructure is comparatively thick, the truck load is resulting in very minor strain which is close to the resolution of the sensors, especially for the fiber optic sensors.

2.4 Effective width of GFRP deck as compression flange (load case 1)

2.4.1 Measured strain distribution

To analyze the effective width of the FRP deck when acting compositely with the steel girders, the strain on the FRP deck soffit in longitudinal direction is being measured. The actual load distribution of each truck has been implied in the FEA analysis and compared to the respective measurement. Close to the northern abutment (GL 10A) the FRP deck is subjected to tension while in the center (GL 15) there is compression in the deck. The position of zero bending moment is between gridlines 12 and 13. While the calculated and measured strain distributions are comparable in general, there are noticeable derivations (Figure 8). In order to better compare the measurement results, the strain of each individual load test had been scaled to the ratio 200 kN / actual truck load. Though the non-uniform load distribution within one truck load cannot be equalized, the values are at least better comparable.

At the abutment (GL 10A) the measured strain distribution is more uniform and in 3 out of 4 load tests the values are higher than predicted with FEA. This might be an indication that the tension force in the deck is directly transferred into the RC abutment, even if there is not adhesively bonded together, but are in contact b/c of internal compression. The one measurement where tension is lower (Nov. 10) was the one with the

lowest ambient temperature. This might be caused from a gap between FRP deck and RC abutment due to colder temperature.

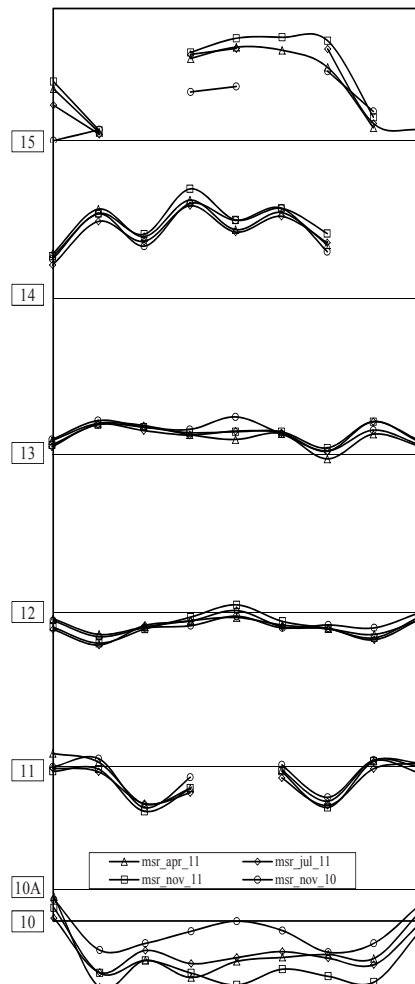


Figure 8: Strain values, scaled to a 200 kN truck

At GL 11 the situation is vice versa: the predicted distribution according to FEA is more uniform than the actual measurements. This means that already 2 m from the abutment, the load is concentrated in the vicinity of the steel girder. The edges show almost zero strain.

The strain values at the bridge center (GL 15) are in very good agreement with the prediction for the 3 other measurements except again the one in Nov. 10, which is quite below the FEA results. In contrast, the distribution of the longitudinal strain is different than predicted: it can be noted that at the edges the strain is smaller than predicted.

Since the rear axle of the truck is located only 1 m from this gridline, the non-uniform distribution is also a result of the concentrated wheel loads. Since the FEA analysis is an exact image of the imposed action, the alteration is a result of a load bearing behavior which differs from the analysis. As it will be discussed in 2.4.2, the Poisson's ratio has a decisive influence on local load distribution.

2.4.2 Variation of FEA analysis input values

Figure 9 shows the influence of the variation of the elastic modulus of the surfacing layer as well the outcome of altering the FRP deck's Poisson's ratio.

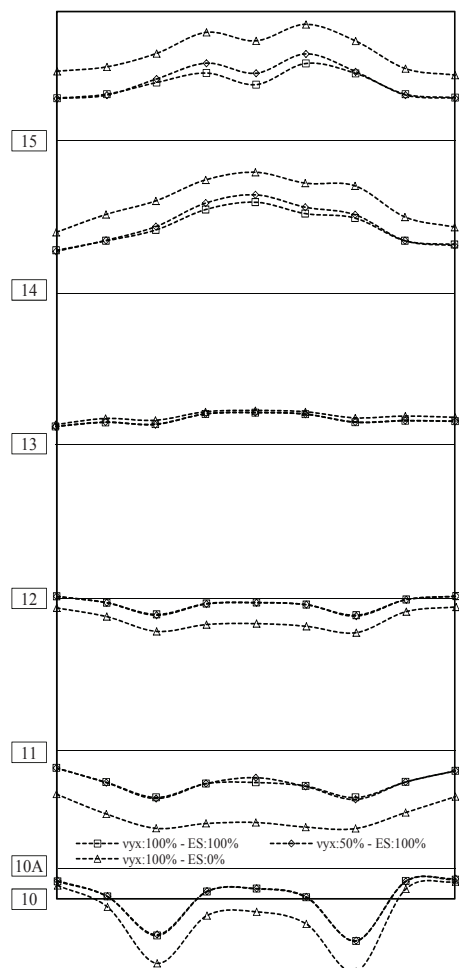


Figure 9: Variation of FEA analysis results depending on values for Poisson's ratio (v_{yx}) and elastic modulus of the surfacing layer (E_s)

As described in 1.3, the input values of the FEA analysis are subjected to uncertainties. The comparison with the measurement results allows for optimization and calibration of the FEA model. First of all, the surfacing layer has a decisive influence on the load bearing behavior, if it will be not taken into account the strain in the FRP deck raises significantly.

A variation in the Poisson's ratios of the FRP materials has no influence in most areas, but significant influence in the vicinity of the concentrated wheel loads (GL 15). With lower values, the strain in the center of the bridge is increasing, while they stay constant at the edges.

2.5 Load distribution in GFRP deck spanning between steel girders (load case 2)

As shown in Figure 6, the decisive load for the investigation of the strain distribution transverse to the bridge span is the rear left wheel (RL). The sensor array is placed between GL 12 and GL 14, on the eastern half of the superstructure. Therefore, the results are being scaled to a virtual load of $F_{RL} = 57 \text{ kN}$ and compared to the results of FEA analysis (Figure 10).

The measurement results vary significantly from the computed prediction. The strain at the eastern steel girder is positive opposed to the FEA results which are slightly negative. At the intermediate sensor row, the strain has the same qualitative distribution as the calculation but considerably smaller values. In the center line of the bridge, the measured results are in good accordance, but one sensor didn't return valuable readings, thus no value can be given for the maximum sagging moment.

Poor modelling can't explain this discrepancy, since the FEA model takes transverse strain and the 3D setup of the FRP deck into account.

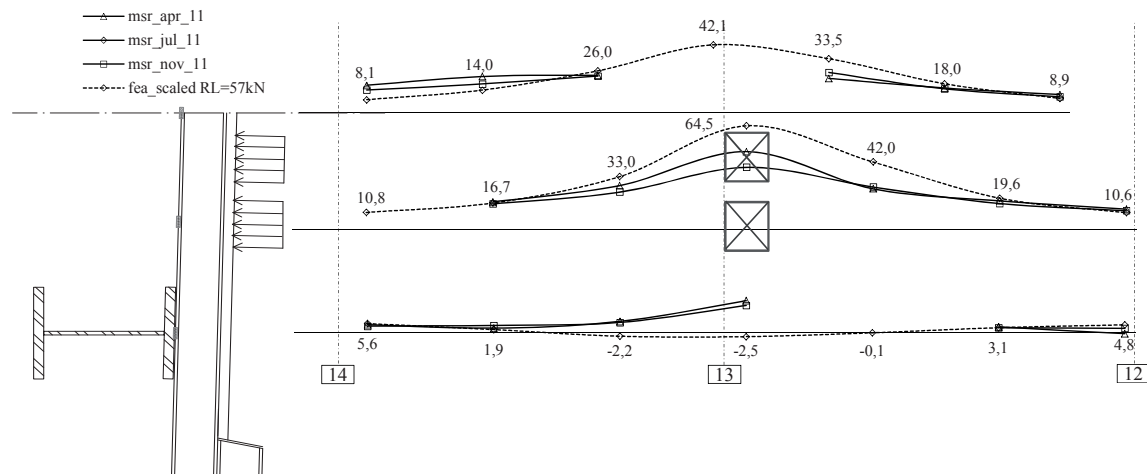


Figure 10: Strain distribution transverse to bridge span due to a virtual wheel load of 57 kN, measurement results and FEA analysis prediction

3 Conclusion

The monitoring of the FRP road bridge in Friedberg shows that all structural details are well operational, especially the crucial adhesive layer between the steel girders and the FRP deck. The two utilized strain sensors – electronic strain gauges and fiber optic sensors deliver the same results, though some of the electronic sensors have been corroded after three years of exposure.

The measured strains are in general smaller than predicted. This is an indication that secondary members such as the surfacing layer or the parapet contribute to the global load bearing behavior. Moreover, the results show that the FRP deck can transfer tension forces directly into the abutment though they are not immediately connected. This behavior might be a result from a superimposed compression in the superstructure due to temperature difference and loading of the backfill behind the RC abutments. The measured tension corresponds to live load only.

4 References

- [1] Knippers, J.; Pelke, E.; Gabler, M.; Berger, D.: Bridges with Glass Fibre-Reinforced Polymer Decks: The Road Bridge in Friedberg, Germany. In: Structural Engineering International 4/2010, pp. 400-404
- [2] Gabler, M.; Knippers, J.: Improving fail-safety of road bridges built with non-ductile fibre composites. In: Construction and Building Materials, Volume 49, 12/2013, pp. 1054–1063
- [3] Keller, T.; Görtler, H.: In-plane compression and shear performance of FRP bridge decks acting as top chord of bridge girders. In: Composite Structures 2/2006, pp. 151-162
- [4] Reising, R. M. W.; Shahrooz, B. M.; Hunt, V. J.; Neumann , A. R.; Helmicki, A. J.; Hastak, M.: Close Look at Construction Issues and Performance of Four Fiber-Reinforced Polymer Composite Bridge Decks. In: Journal of composites for construction 1/2004, pp. 33-42
- [5] Lee, S. W.; Hong, K. J.; Park, S.: Current and Future Applications of Glass-Fibre-Reinforced Polymer Decks in Korea. In: Structural Engineering International 4/2010, pp. 405-408
- [6] Wattanadechachan, P.; Aboutaha, R.; Hag-Elsafi, O.; Alampalli, S.: Thermal Compatibility and Durability of Wearing Surfaces on GFRP Bridge Decks. In: Journal of bridge engineering 4/2006, pp. 465-473



Application of GFRP for Bridge Inspection Way

Yoshiyasu FURUYA, Takeshi HIROSE

Nippon Expressway Research Institute Company Limited, Tokyo, JAPAN

Hitoshi NAKAMURA, Yuya ISHII

Tokyo Metropolitan University, Tokyo, JAPAN

Kousuke KOIZUMI

East Nippon Expressway Company Limited, Tokyo, JAPAN

Contact: y.furuya.aa@e-nexco.co.jp

Abstract

This paper reports on the results of tests conducted to verify the applicability of bridge inspection way using glass fiber-reinforced polymer (GFRP). The process of setting the Japanese expressway standards for fiber-reinforced polymer (FRP) bridge inspection way is also described in this paper.

The proposed bridge inspection way adopts lightweight and highly anti-corrosive GFRP. The bridge inspection way consists of GFRP slab panels that sandwich hard urethane foam and truss girders that serve for railings to further reduce its own weight.

Nippon Expressway Company Limited (NEXCO) have also established standards for FRP bridge inspection way installed on Japanese expressway bridges, based on the knowledge obtained from development of bridge inspection way, literature reviews and case studies in Japan.

Keywords: Fiber-reinforced polymer, bridge inspection way, sandwich-panel floor slab, pony-truss type, establish standards

1 Introduction

Construction of expressway in Japan began in the 1960s, and deterioration is progressing as expressway age. What is required, now, of road operators in Japan is to maintain these road structures efficiently. Recently, it has become mandatory [1] in Japan to visually inspect bridges every five years. Visual inspection requires inspectors to check the bridges at close range,

which means that there are strong needs for bridge inspection way.

Typical bridge inspection way uses economical steel members and applies hot-dip galvanizing to prevent corrosion. However, the anti-freezing admixture is sprayed on Japanese roads in winter to prevent freezing, which sometimes causes the steel bridge inspection way to corrode.

To counter this problem, a bridge inspection way using GFRP as a structural material is being

developed. Now, existing GFRP inspection way were basically designed as a girder structure using channel members, same as the steel inspection way. This structure is not rational because the elastic modulus of GFRP is low. To increase the rigidity of GFRP bridge inspection way, we tried adopting the pony-truss girder and using a sandwich-panel floor slab with ultra light weight core material. By combining these elements, we have developed a GFRP bridge inspection way that is advantageous in structural and cost performance.



Fig. 1: Damage on a steel inspection way

2 Development of bridge inspection way with sandwich-panel and truss girder

2.1 Design conditions

Table 1 shows the design conditions of inspection way.

There was no standard deflection limitation set for the way, so we used that for pedestrian bridges.

Inspectors need to wear a safety belt when inspecting. The safety belt must pass an impact resistance test using a sandbag weighting 85kg, to secure safety of the inspectors.

So a standard for the handrail of the inspection way was established referring to that of the safety belt. A safety belt is connected to the handrail and the sandbag is dropped from the way, to confirm that the sandbag does not drop to the ground.

In Japan, there were no standards for GFRP bridge inspection way, and manufacturers made and installed inspection way based on their own standards and R&D. For this reason, users raised concern about the safety and quality of the products. The cost of the inspection way also varied from maker to maker.

Therefore, based on the knowledge acquired through R&D of GFRP inspection way and the standards for steel inspection way, new standards for FRP bridge inspection way was established for Japanese expressway.

Table 1: Design condition of inspection way in this study

Item	Reference value
Design live load	3.5 kN/m ²
Deflection limitation under design live load	$L/400$
Limit on natural vibration	Outside the range of 1.5 to 2.3 Hz
Vertical load on handrail	0.59 kN/m
Horizontal load on handrail	0.39 kN/m
Limit by static loading test on handrail	Under breaking strain
Applicable span length L	Under 9.8 m

2.2 Structural detail

2.2.1 Structure, material and dimensions

Table 2 shows the structural details and Fig. 2 is a general view of the truss girder type bridge inspection way used in the tests. The span lengths

were set at 5.8 m and 9.8 m. The 5.8 m span was adopted because the length is used for cross-beams in typical multi-girder steel bridges, designed using old Japanese standards. We suppose that its length covers almost expressway bridges. The 9.8 m length was set considering the maximum span length under the current standards.

For the upper cord, lower cord, diagonal member, and vertical member, pultruded GFRP channels of C75 ($H75 \times B40 \times t5.0$ mm) are used. For non-structural connecting beams, pultruded GFRP square pipes of SP60 ($H60 \times B32 \times t4.0$ mm) are used.

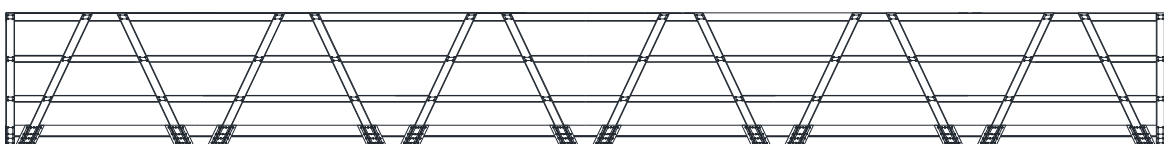
The inspection way is made of sandwich panel floor slab, shown in Fig. 3. It consists of two GFRP channels of C75 as lower chord, placed on both sides. The 3mm-thick continuous-molded panels, with hard urethane foam sandwiched between the two panels as core material, is fixed on the top and bottom faces. Both edges of the floor slab top

have toe-plates that will work to prevent instruments and tools from falling off during inspection. The toe-plate was cut out from GFRP channels of C100 ($H100 \times B50 \times t5.0$ mm).

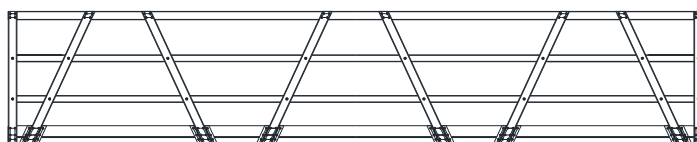
The panel points will be connected using blind rivets and adhesive, a method that can join members efficiently, and the typically applied method of using gussets will not be employed. This method was selected because the cross sections of channel were small, members should be directly bonded each other, and because connection by one side should be required for closed section. Based on previous study [2], stainless steel (JIS SUS305) blind rivet (Diam. 4.8mm) is selected. And stainless steel (JIS SUS304) M6 bolt was also selected, considering the fabrication of members in situ and the replacement of damaged handrails.

Table 2: Structural detail

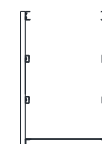
Item	Design value/ reference value
Effective width	0.6 m
Handrail height	1.1 m
Distance between vertical struts	1.9 m or less



a) 6-panel model with span length 9.8m



b) 3-panel model with span length 5.8m



c) Cross section

Fig. 2: General view of truss girder type inspection way

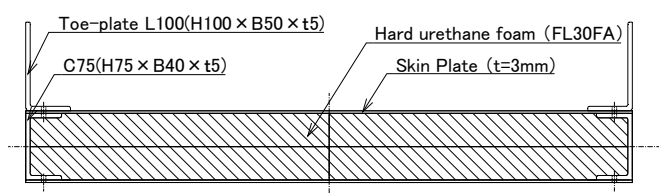


Fig. 3: General view of sandwich panel floor slab

2.2.2 Adjusting span length

A diagonal member with the bracing angle of 65° was adopted to reduce mistakes and costs in fabrication. However, the constant angle of bracing is limited for variable span length. Regarding such a problem, the extension of the interval between panel points is proposed and we have conducted loading tests on models with the different panel lengths and the constant angle of bracing. The model with span length 5.8m as shown in Fig. 2 would be suitable for 4 panels, but the loading tests were carried out using a 3-panel model. The test results confirmed that span lengths of 2.3m to 10.0m are applicable by adjusting the panel lengths.

2.3 Verification of serviceability and safety

To examine serviceability and safety, the deflection of slab panel under static live load, the vibration serviceability caused by dynamic load, the safety of handrails under static lateral and vertical load and impact load considering the accidental fall of inspectors were investigated

experimentally. All tests have satisfied the requirement.

2.3.1 Deflection of inspection way

Loading tests under design live load were examined to check the serviceability of deflection in inspection way. The design live load was statically applied for the GFRP panel slab, and sandbags equivalent to about 3.5kN/m² were used. And the vertical deflections on the bottom side were measured.

The real size models with 5.8 m span length and 3 panels, and another with span length of 9.8 m and 6 panels were fabricated for loading tests. Fig. 4 shows the distribution of vertical deflections. The maximum deflection for 5.8m span length, 3-panel model was at the center of span and was 7.76 mm (1/747). The maximum deflection for span length 9.8 m, 6-panel model, was also at the center of span and was 17.47 mm (1/561). These tests confirmed that the proposed inspection way satisfy the value of deflection limitation ($L/400$) applied on pedestrian bridges in Japan.

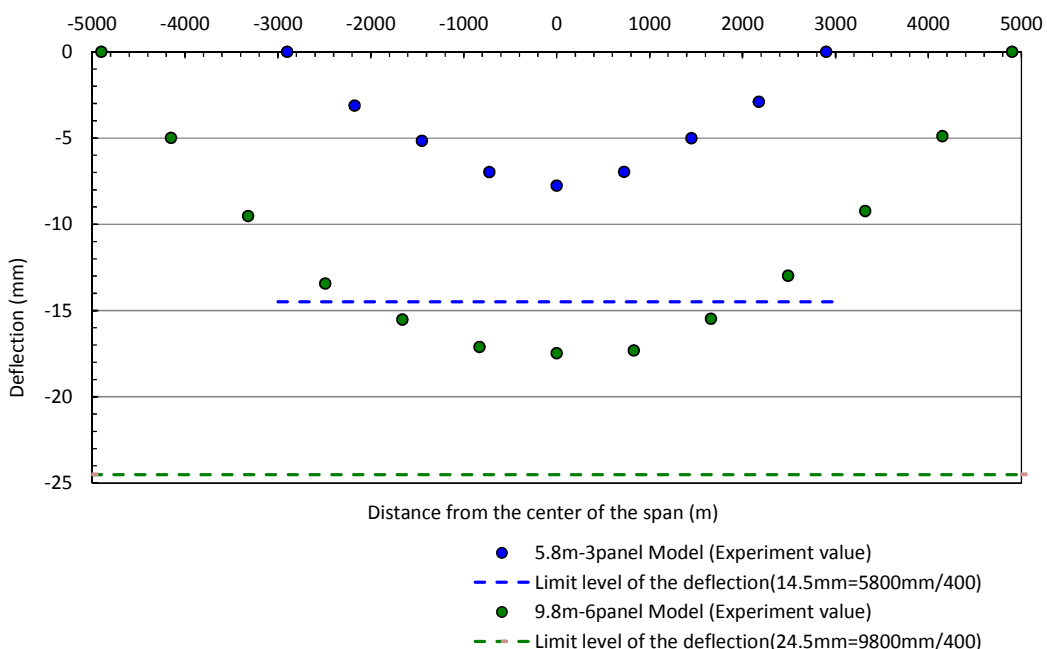


Fig. 4: Distribution of vertical deflection (indicated in graphs for 5.8 m and 9.8 m)

2.3.2 Deflection of inspection way

Vibration tests on inspection way were examined to check the vibration serviceability. The vibrations were caused by free-falling of a 20-kg sandbag at the height of 1.1 m and natural frequencies were measured using accelerometer. The first natural frequency was 17.8 Hz for span length 5.8 m and 11.9 Hz for span length 9.8 m, respectively. It was confirmed that both span lengths satisfy the vibration serviceability (outside the range of 1.5Hz to 2.3Hz).

2.3.3 Safety of handrail under static load

To check the safety of handrail, its strain was measured under static load, considering that workers will lean on or step on the handrail.

As the vertical load, sandbags equivalent to 0.59 kN/m were placed between the panel points of the upper chord, and the maximum strain of the members were measured. As the horizontal load, a screw jack was used to statically apply the concentrated load equivalent to 0.39 kN/m on the panel point of the upper chord, and the maximum strain of the member were also measured.

Table 3 shows the test results of span length 5.8 m, 3-panel model as a typical example. It was confirmed that the measured strains were significantly small against failure strains. These tests confirmed that the proposed inspection way satisfy the value of deflection limitation applied on pedestrian bridges in Japan.

2.3.4 Safety of handrail under impact load considering the accidental fall of inspectors

To check the safety of handrail under impact load considering the accidental fall of inspectors, a sandbag weighing 85 kg was connected to the handrail via a safety belt. The sandbag was dropped from the height of the upper chord and the damage to the handrail was investigated. It was assumed that safety belts may be fastened on places other than the upper chord and the test was carried out by dropping a sandbag attached to the horizontal bar via a safety belt, and the damage to the handrail was checked.

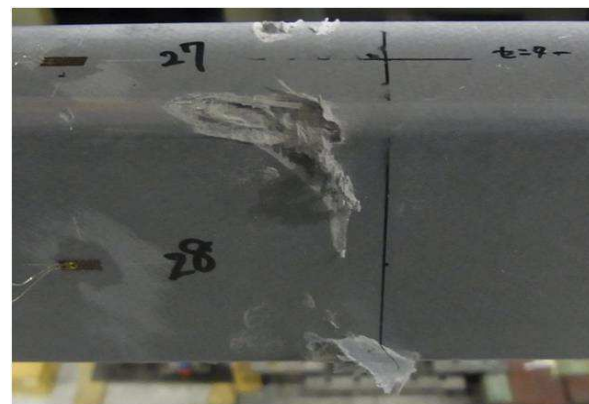
Fig. 5 shows damage to the span length 5.8 m, 3-panel model as a typical example. Although damages were partially occurred ,the handrail prevented the sandbag from falling to the ground.

Table 3: Maximum strain of handrail

Item	Measured strain $\varepsilon_e (\times 10^{-6})$	Failure strain $\varepsilon_u (\times 10^{-6})$	$\varepsilon_u/\varepsilon_e$	Location with Maximum strain
Vertical load (5.8m, 3-panel)	134	15,000	112	Handrail
Horizontal load (5.8m, 3-panel)	-671	15,000	22	Support
Vertical load (9.8m, 6-panel)	146	15,000	103	Handrail
Horizontal load (9.8m, 6-panel)	-1,284	15,000	12	Support



a) Upper chord



b) Horizontal bar

Fig. 5: Damages to handrail after impact loading test

2.4 Summary

Test results were summarized as follows:

- 1) 2 types of inspection way were tested applying a load of 3.5 kN/m^2 . For deflection limitation $L/400$, it was $1/747$ (maximum deflection 7.76 mm) with span length 5.8 m, 3-panel model. With 9.8 m, 6-panel model, it was $1/561$ (maximum deflection 17.47 mm). These values confirm that the proposed inspection way has sufficient high rigidity.
- 2) Based on vibration test the natural frequency of the panel slab was outside the limit value of 1.5 to 2.3 Hz, and it was confirmed that the natural frequency satisfies the vibration serviceability.
- 3) Loading tests were carried out by applying vertical load (0.59 kN/m) and horizontal load (0.39 kN/m) on the handrail. It was confirmed that the maximum strain was sufficiently smaller than the failure strain.
- 4) By impact loading test considering the accidental fall of inspectors, it was confirmed that although the handrail was partially damaged, it did not break.

It was confirmed that the sandwich-panel, truss girder type bridge inspection way satisfied all design requirements. The bridge inspection way developed weighs only 29.4 kg/m and is very light, weighing 37% less than conventional steel bridge inspection way.

3 3. Setting the standards for FRP bridge inspection way

As mentioned above, there are strong needs for bridge inspection way. However, conventional steel inspection way may corrode and deteriorate depending on the environment of the installed location, putting inspectors in danger.

To secure durability of inspection way installed in a corrosive environment, FRP bridge inspection way were needed. But Japan had standards only for steel inspection way, and these standards were difficult to apply to FRP inspection way; so new standards were required.

3.1 Standards for conventional bridge inspection way

To set the new standards, we studied standards for steel inspection way. Japan has standards only for steel bridge inspection way and they are shown in Table 4. Structural details are decided through structural calculation using the allowable stress. The safety factor is set at about 1.7 for yield strength, referring to the standards for road bridges. The deflection limitation under live load was calculated based on case studies. The deflection limitation was about $L/300$.

Table 4: Basic structure/design load for steel inspection way

Item	Design/ reference value
Effective width	0.6 m
Handrail height	1.1 m
Distance between vertical struts	1.9 m or less
Design live load	3.5 kN/m^2
Vertical load on handrail	0.59 kN/m
Horizontal load on handrail	0.39 kN/m

3.2 Standards for pedestrian bridge

We studied standards for pedestrian bridges that are structurally similar to bridge inspection way. The standards for pedestrian overpasses in Japan are shown in Table 5. Guidelines for design and construction of FRP footbridges[4] are available, and deflection limitation should be selected for construction situation.

Table 5: Basic structure/design load based on Standards for pedestrian bridge

Item	Design/reference value
Effective width	1.5 m and over
Handrail height	1.0 m and over
Distance between vertical struts	-
Design live load	3.5 kN/m ²
Deflection limitation under design live load	$L/600$ (<i>May be allowed to $L/400$ if vibration serviceability is satisfied</i>)
Vibration serviceability	Not uncomfortable for users (outside the range of 1.5 to 2.3 Hz)
Vertical load on handrail	1.0 - 1.5 kN/m
Horizontal load on handrail	2.5 kN/m

3.3 Survey of existing FRP inspection way

The survey was conducted for setting the new standards to check inspection way already installed on expressway bridges. As there were no standards for FRP inspection way in Japan, manufacturers have studied the reasoning behind setting the design load, the value of deflection limitation, impact performance on handrail and other such factors, using various methods, and established their own standards.

A major difference between the standards of each manufacturer was in the design load and deflection limitation. One maker considered that inspections are typically carried out in pairs, and so they studied concentrated live load and not full live load, and set the load at 1.5 kN and the deflection limit at $L/400$.

3.4 Proposed standards for FRP bridge inspection way

The new standards are shown in Table 6. The effective width, handrail height, and length between vertical struts are the same as the steel inspection way.

Design live load and vertical and horizontal load on handrail for steel inspection way were adopted for the FRP inspection way. The values of vibration

serviceability and deflection limitation that do not cause uncomfortableness for workers were investigated.

The deflection limitation of the main girder under design live load was set at $L/100$. The reason was as follows: The design live load of 3.5 kN/m² is equivalent to the loading condition positioned a weight of 85 kg every 40 cm. This is a very rare case, so the loading condition were simulated to confirm the degree of deflection that user feel uncomfortable when using actually. It was found that the deflection limitation of $L/400$ may be satisfied under actually using even if the deflection limitation is allowed to $L/100$ or smaller under the design live load of 3.5 kN/m², and that the value of deflection limitation does not cause users to feel uncomfortable.

The vertical and horizontal load on handrail were adopted based on Standards for steel inspection way. The impact loading test was also defined to check the load carrying capacity of handrail in case a worker wearing a safety belt falls off. The criteria for safety were that damage to handrail is allowed but a worker falling to the ground is not acceptable.

Table 6: Basic structure/design load

Item	Standards for expressway bridge inspection way
Effective width	0.6 m
Handrail height	1.1 m
Distance between vertical struts	1.9 m or less
Design live load	3.5 kN/m ²
Deflection limitation under design live load	$L/100$
Vibration	Outside the range of 1.5 to 2.3Hz
Vertical load on handrail	0.59 kN/m
Horizontal load on handrail	0.39 kN/m
Impact load on handrail	Doesn't fall at approx. 8 kN impact load

4 Conclusion

The proposed GFRP bridge inspection way with sandwich-panel and truss girder is an innovative inspection way. Test results showed that span length could be extended up to 9.8m. It was also confirmed that the inspection way weighs 29.4 kg/m and is light weight.

The standards for expressway bridge inspection way have been established in Japan based on case studies, R&D of FRP inspection way and literature reviews.

The test results of the GFRP bridge inspection way with sandwich-panel and truss girder for new standards showed that the proposed inspection way satisfies the requirements.

References

- [1] Recommendations for Full-scale Maintenance of Aging Roads: Ministry of Land, Infrastructure, Transport and Tourism, The Road Committee of the panel on Infrastructure Development, Japan, 2014.
- [2] Nobuhiko Kitayama, Ken-ichi Maeda, Hitoshi Nakamura, Tesuya Watanabe, Hideki Setouchi: Development of girder connection using rivet and structural adhesive in a GFRP pedestrian slab bridge, Journal of Structural Engineering, Vol.59A, pp.936-948, Japan, 2013 (in Japanese)
- [3] 2Level crossing facilities technical standards, the commentary: Japan road association, Japan, 1979. (in Japanese)
- [4] Guidelines for Design and Construction of FRP footbridges: Japan Society of Civil Engineers, Hybrid Structure Series 04, 2011. (in Japanese)
- [5] Yoshiyasu Furuya, Hitoshi Nakamura, Hiroshi Nakai, Kousuke Koizumi and Masayuki Nishida: Development of bridge inspection path using GFRP trussed girder, FRPRCS-12 /APFIS-2015, 2015.
- [6] Hitoshi Nakamura, Kousuke Koizumi, Yuya Ishii, Yoshiyasu Furuya, Hiroshi Nakai and Masayuki Nishida: The structural characteristics on a bridge inspection path using GFRP trussed girder, FRPRCS-12/APFIS-2015, 2015.

Application of FRP Materials for Construction of Culvert Bridges

Jincheng Yang, Reza Haghani

Chalmers University of Technology, Gothenburg, Sweden

Contact: reza.haghani@chalmers.se

Abstract

Steel culvert bridges have been used for almost a century. The attractiveness of this type of bridges is usually attributed to their low initial investment, fast manufacture and installation, and their geometrical adaptability. Despite the advantages offered by steel culverts, they might suffer from a number of drawbacks in certain conditions, for instance, in case they are in direct contact with water. The most common problems are corrosion and abrasion of galvanized steel coating and fatigue. Fiber reinforced polymer (FRP) materials offer advantages such as very high specific strength and stiffness, very good durability and fatigue resistance, and light weight. Therefore, there has been a great deal of interest in using FRP composites in construction industry in the past decade. This paper presents the results of a study on feasibility of using FRP composite materials for manufacture of culvert bridges as an alternative for steel. Different aspects such as design of FRP culverts, manufacturing issues and life cycle costs are discussed.

Keywords: Steel; Fiber reinforced polymer; Culvert; Bridge; Durability; Fatigue; Life cycle cost.

1 Introduction

The concept of corrugated steel pipe profiles was presented in the mid 1950's. The design was based on primitive diagrams and standard drawings, addressing two types of conduits only: low-rise culverts and vertical ellipses. By then, the standard drawings were only applicable for the structures with spans up to 5 m. However, several culverts with a span over 5 meters were also erected.

With advancements in knowledge about culverts and technology related to these structures, more advanced and accurate design methods were developed, capable of considering different parameters for soil material, larger spans and various cover heights.

Steel culvert bridges can be defined as flexible corrugated structures forming a pipe or an arch shape. These structures gain their load bearing

capacity by the interaction between conduit wall and the surrounding soil. A common configuration of a culvert bridge is illustrated in Figure 1. The extensive usage of culverts can be attributed to their advantages such as (1) low initial cost, (2) fast manufacturing and assembly, (3) aesthetics: natural exterior because of the overfill, (4) simple construction, and (5) adjustment to possible extension or widening of the road.

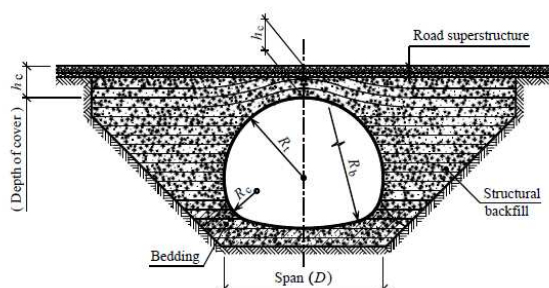


Figure 1. Typical configuration of a corrugated steel pipe arch culvert [1]

The performance of a culvert bridge is highly dependent on a thorough soil compaction, therefore great attention should be paid to proper backfill [5] in order to obtain adequate strength, prevent wash-outs and settlements.

The selection of a culvert shape is based on: 1) the site conditions, such as span and cover height, 2) flow capacity and fish passage for the river-passage culvert bridges. The proposal should also be cost-effective and durable. Culvert bridges are mainly classified as: (1) closed profiles and (2) arch-type profiles. Culvert bridge structures can function as pedestrian, highway, railway and road bridges as well as for the passage of water and traffic via conduit.

The first full-scale test of a pipe arch was performed by The Royal Institute of Technology (KTH) in 1983 supported by Swedish Road Administration [4]. The structure had a span of 6.1 meters with a cover height of 1 meter. The tests were followed by a proposed Swedish design method in 2000. Thereafter, The Swedish Road Administration (Vägverket) implemented the method in the code Bro 2002, and the National Rail Administration (Banverket) accepted it in "BV Bro".

There exist about 4430 culvert bridges in Sweden, among which 4100 are made of steel according to Swedish Bridge and Tunnel Management system (BaTMan) [2]. The common span length for culverts in Sweden is 5 meters or less [3].

According to Swedish Bridge Design Code "TRVK Bro 11" (2011) culverts are commonly designed for the technical life of 80 years; however culverts are constantly exposed to adverse environment, thus making the inspection and maintenance frequent and service life shorter.

The vast majority of culverts around the world were built in 50's and 60's, and thus road authorities deal with a large stock of old culverts. Many culvert bridges in Sweden have deteriorated to the point where replacement or repair is warranted.



Figure 2. The field test of a pipe arch culvert in Sweden [4]

2 Problem definition

As mentioned previously, culverts can be used in a variety of conditions, for instance as a road bridge crossing a stream, aquatic fauna passage and drainage purposes. Thus, the most concerning issue is the corrosion (see Figure 3), which has a significant effect on service life of the structure. The most exposed location and prone to deteriorate, is the invert (see Figure 4). In addition, the damage of protective layer due to road salts might appear especially in aged structures, allowing corrosion and annihilation of the base metal. Eventually, increased traffic and improper maintenance can lead steel culverts to become structurally deficient and/or functionally obsolete.

Available measures for dealing with corrosion problem in steel culvert bridges mainly include shotcreting of the internal walls, partial or complete relining of the culvert (in case of more severe damage, see Figure 5) and finally total replacement of the culvert.

Another problem, which might take place individually or hand-in-hand with corrosion is the fatigue resulted from traffic loads. Steel FRP culverts are normally produced as individual corrugated steel plates, assembled on site using bolted connections. The presence of holes, and thus fatigue prone details, sometimes governs the structural design of the culvert and can cause some problems during the service life of the structure.



Figure 3. Corrosion in a corrugated steel culvert [5]



Figure 4. Deteriorated invert and perched end of pipe culvert [6]



Figure 5. An entire culvert re-lining in Buffalo, New York, USA [7]

With regard to above mentioned problems, structural solutions providing more durable structures which need less maintenance is highly appreciated by road authorities and bridge owners.

3 Fiber reinforced polymer (FRP) materials

The history of composites can be tracked back thousands of years ago to ancient Egypt where the straw fibers were used as a reinforcement in mud bricks. The first application of modern synthetic fibers took place in the early 1930's, when short glass fiber were used in cement as a reinforcement in the United States. The development of fiber reinforced polymer, with the composition that we know today, started in the early 1940's when advanced polymers emerged.

As the name of the material suggests, FRP is composed of two constituents: high-strength fiber embedded in a polymer matrix, giving a high-performance composite material. After World War II, during which FRPs were used mainly in defense industries, the polymer-based composites spread broadly when the fiber reinforcements and resins became commercially available and affordable. Primarily, FRP automotive industry introduced composites into vehicle frames in early 1950s.

The greatest advantages of FRP composite materials include: (1) very high specific strength and stiffness, (2) light weight, (3) good durability and corrosion resistance, (4) tailor-ability and resilience, and (5) sustainability due to less embodied energy compared to conventional construction materials such as steel and concrete.



Figure 6. Example of using FRP composites in construction of a pedestrian bridge, manufactured by Fiberline, Kolding, Denmark [8]

FRPs were introduced to construction industry in mid-70th where they were used for strengthening and repair purposes. Superior mechanical properties of FRPs combined with advantages offered by adhesive bonding, created an effective and efficient solution for upgrading of infrastructure and tens of thousands of structures have been strengthened and repaired using this

technique since that time. After almost four decades, progress in materials knowledge and manufacturing techniques and also price has enabled manufacture of structures such as bridges from FRP materials, see Figure 6. At the present, FRP materials are used in a wide range of applications in construction industry, from manufacturing door and window frames to manufacture of superstructure of road bridges.

4 Feasibility of using FRP composites for manufacture of culvert bridges

In order to investigate the feasibility of using FRP composites for construction of culvert bridges, the study was divided into three phases. The first phase included the overall design of a culvert bridge with a reasonable span. The aim of this phase was to get the approximate dimensions of sections and evaluate whether they are within reasonable range for manufacturing. In the second phase, possible manufacturing methods, with regard to obtained dimensions, were investigated to ensure manufacturability. In the third phase, a LCC analysis was performed to prove the economic feasibility of the structure with regard to an equivalent steel culvert.

4.1 Structural design of the FRP culvert

To carry out the first phase of the study, an existing steel culvert bridge was chosen. After obtaining the overall dimensions of the bridge (i.e. span and height), the design of an equivalent FRP structure was carried out. The reason for selecting an existing project was to facilitate the LCC comparison in phase 3 of the study. The selected culvert, is located in Rörbäcksnäs, Sweden. An overview of the bridge and the overall dimensions of the bridge are shown in Figure 7 and Figure 8. The bridge carries road traffic over a water passage. The box-shape steel culvert has a span of 12.4 meters. Extra reinforcement layers are added to the crown and two corner sections as illustrated in the Figure 8. The width of the bridge is 10 m and the total length is 27 m. The bridge has an average daily traffic (ADT) of 136 vehicles and 10 trucks (registered in 2004).

It was decided to use FRP sandwich panels in the structural design due to high stiffness and rigidity

of such panels. The loads on the structure were determined from EUROCODE, and EUROCOPM (Design code and handbook) was used for the design of FRP panels. As the existing codes and guidelines mainly address the design of corrugated steel culverts, and no calculation methods exists for FRP structures, it was decided to use finite element method for the design. Commercially available software ABAQUS, ver. 6.13 was used for this purpose (Figure 10).



Figure 7. Case study culvert bridge, a box culvert bridge over Siktån river at Rörbäcksnäs, Sweden (Picture from BaTMan [2], bridge number 20-1335-1)

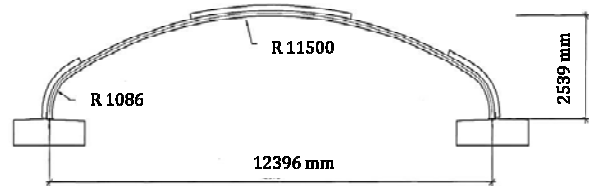


Figure 8. Geometry and dimensions of the steel culvert structure with box profile used in Rörbäcksnäs bridge

Due to lower price of glass fibers, compared to other typical fibers such as carbon, it was decided to use glass fibers in combination with epoxy resin for manufacture of FRP panel skins. Polypropylene honeycomb was selected to be used as core material. E-glass fibers with modulus of elasticity equal to 70 GPa and Poisson's ratio of 0.22, and epoxy resin with modulus of elasticity equal to 3.2 GPa and Poisson's ratio of 0.36 were used. The fiber volume fraction was 45% while all the fibers were laid in 0° direction (load bearing direction).

Design of the culvert structure, was carried out using commercial FE program Abaqus, ver. 6.13. Linear solid elements were used for all parts of the models. The soil-FRP interface behavior was defined by hard contact-frictionless interaction.

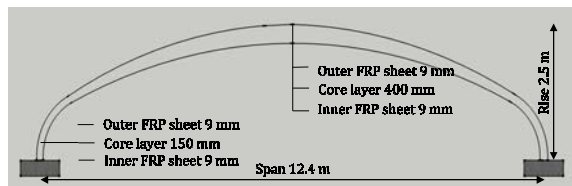


Figure 9. Geometry and dimensions of the FRP culvert for the case study bridge

The sandwich panels consisted of 9 mm skins in the inner and outer faces. The thickness of the panel varies from 150 mm, at the base of the arch, to 400 mm, at the crown of the arch (Figure 9). The finite element model, used for design and optimization is shown in Figure 10.

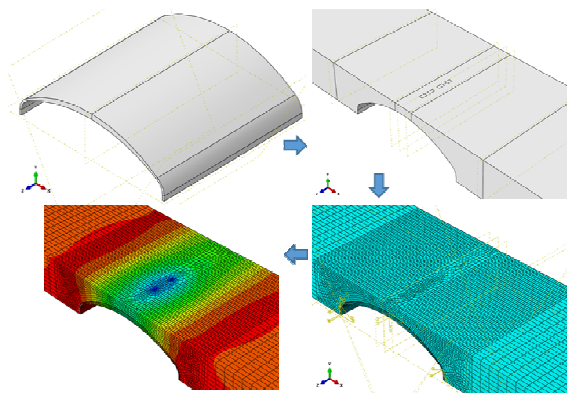


Figure 10. Finite element model in Abaqus

4.2 Manufacturing of FRP culverts

There are a number of methods for manufacturing large scale FRP segments namely: (1) pultrusion, (2) resin infusion, and (3) filament winding. Among these methods, resin infusion is the only feasible method to manufacture the panels mentioned above. In this method, dry layer of fiber fabrics, according to the design, are stacked on the formwork which will form the bottom skin of the panel. Then the core material will be laid down and finally above procedure will be repeated to form the top skin. The whole element will be then covered by a plastic sheet. The edges of the sheet will be sealed by special tape. Vacuum, then, will be applied inside the bag to facilitate the resin infusion which will be done through a multiple of inlets to the system. After curing of the adhesive the plastic bag would be removed and the panel could be detached from the mold. This procedure is illustrated in Figure 11.

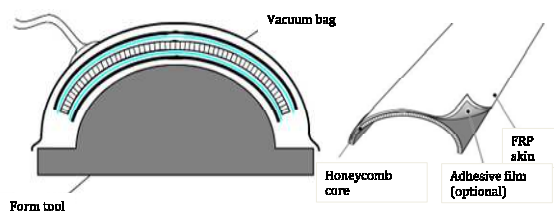


Figure 11. Manufacture of curved sandwich segments using infusion technique [9]

The general construction idea is first to build FRP sandwich segments and then bond the segments to form a culvert structure on construction site as shown in Figure 12.

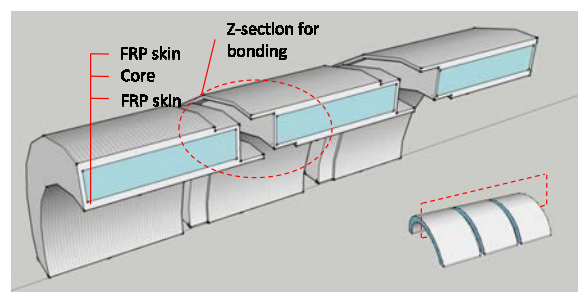


Figure 12. Adhesive joints used to bond FRP sandwich segments

4.3 LCC analysis of FRP culvert case study

In general, LCC analysis serves as a good support for decision-making during bridge management processes. For culvert bridge projects in specific, LCC analysis is helpful to investigate the potential saving since the long-term-cost from maintenance and repair activities of conventional steel culverts forms a significant portion of the total life-cycle cost [6].

The traditional tendering is often based on the lowest bid which is associated with the lowest investment cost of a project. In advanced tendering programs, however, it is not only the cost during investment phase to be considered but also the cost during the service life. In this regard, the LCC analysis, is considered as a primary tool to evaluate the whole life-cycle costs.

Different life-cycle phases include different aspects of cost, influencing the total LCC. They can be categorized into agency costs, user costs and society costs [10], [11]. LCC categories with more details are shown in Figure 13.

In the LCC analysis of the case in this study, both the agency costs and user costs are considered from the investment phase, through the operation and maintenance (O&M) phase, till the end-of-life.

The operation and maintenance phase, which counts from the inauguration to the demolition, includes the activities applied to the bridge for inspection, operation, maintenance, repair, rehabilitation and replacement [10]. The social cost is not considered in the scope of this study.

The life span of the FRP culvert in this study was considered to be 100 years, while the design life of the steel culvert bridge was 80 years. Due to different life spans, the equivalent annual cost (EAC), rather than the net present value (NPV) method, was used to make comparisons between the LCC of the two alternatives [10]. The discount rate in this study was assumed to be 4%.

The results of the LCC analysis have been summarized in Table 1. It can be seen that the FRP culvert bridge results in an annual saving of ca. 2337 EUR and a saving ratio equal to 7% compared to the equivalent steel culvert. The FRP alternative will result in a net saving of ca. 57267 EUR. Further information regarding the LCC analysis is presented in [12].

Table 1. LCC analysis results expressed as EAC

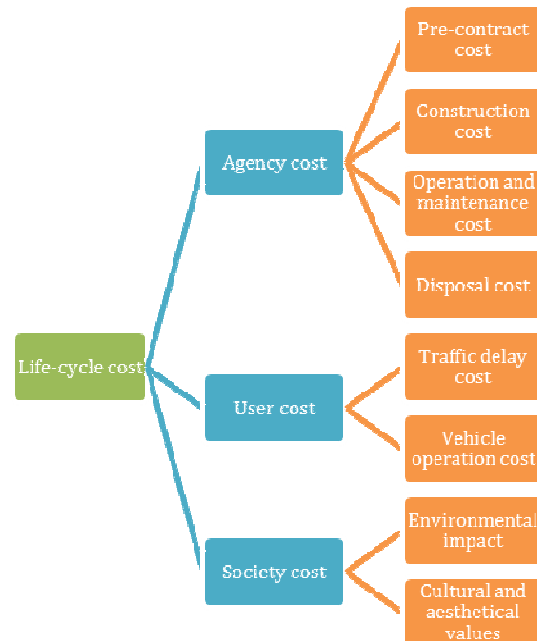


Figure 13. Categories of LCC

5 Sensitivity analysis

Even though the abovementioned conclusions are based on LCC analysis of a real case, the uncertainty in assumptions always exists. In order

Result in EAC	Steel culvert	FRP culvert	Annual Saving	⁴ Saving ratio	⁵ Net Saving
¹ Investment cost	33 548	31 660	1 889	6%	46 285
² O&M cost	2 290	1 889	401	21%	9 824
³ Disposal cost	88	41	47	116%	1 158
Total LCC	35 926	33 589	2 337	7%	57 267

¹Investment cost—Cost during the investment phase, and both agency cost and user cost are included.

²O&M cost—cost during the O&M phase, and both agency cost and user cost are included.

³Disposal cost—cost paid by agency at the end of service life.

⁴Saving ratio—the ratio of annual saving to EAC of the cost-efficient alternative, which is Alternative FRP in the case study according to the LCC results.

⁵Net Saving—the total amount of saving during the life span of the cost-efficient alternative accumulated by annual saving

The values are in EURO.

to add more credit to the LCC analysis, a sensitivity analysis was carried out to investigate the impact of variability in two important parameters on the overall results. These parameters include (1) the price of FRP culvert and (2) expected life span of FRP culvert.

5.1 The price of the FRP culvert

The price of culvert structure can result in significant changes in LCC results. A sensitivity analysis was performed to investigate how the price of FRP culvert structure influences the cost-benefits of the FRP alternative.

The price of FRP culvert structure plays a critical role in determining which alternative is more cost-efficient. In the primary LCC analysis, the price of the FRP culvert bridge was estimated to be 41496 EUR [12], which results in 7.0% saving compared to the steel alternative. The result of the analysis is presented in Figure 14. It can be seen that if the price of FRP culvert structure goes beyond 98493 EUR, the FRP alternative will no longer be competitive and the steel alternative becomes cheaper.

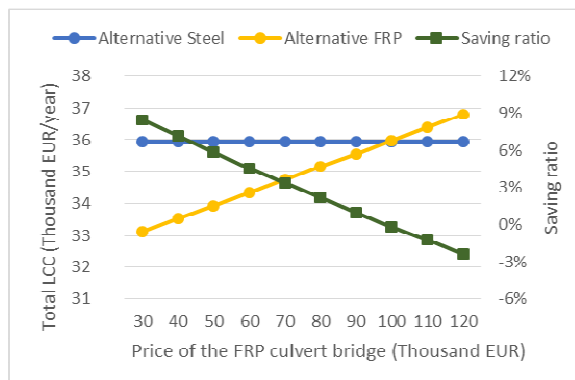


Figure 14. Impact of FRP culvert structure price on the investment cost and saving ratio

5.2 Design life span of the FRP culvert bridge

The design service life of the existing steel culvert bridge is 80 years, which results in a LCC of 35926 EUR/year. When it comes to the FRP culvert structure, a concern is the uncertainty in the design service life and its impact on the LCC. The sensitivity analysis, Figure 15, shows that the FRP alternative can achieve a lower LCC as long as the

life span is longer than 63 years. Otherwise, the steel alternative would become more cost-efficient. Assumption of a minimum life span of 80 years is reasonable and it is believed that FRP structures can reach a life span of +100 years.

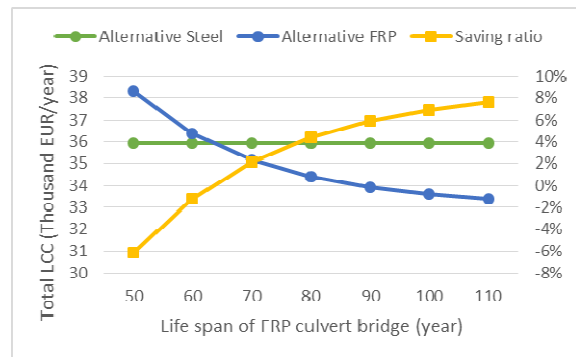


Figure 15. Impact of FRP culvert bridge life span on the total LCC and saving ratio

6 Conclusions

From the results above, the cost benefits of the FRP alternative are clearly seen by comparing the EAC values and the saving ratio throughout all life-cycle phases:

- In terms of investment cost, the saving ratio of FRP alternative is 6 percent (Table 1), which, excluding the impact of longer life span, results from: (1) the cheaper FRP culvert structure and (2) thinner soil cover above the FRP culvert structure. Considering that the investment cost of the steel alternative (2970 EUR/m²) is 61% higher than the average level (1840 EUR/m²) (Indicated by BaTMan as an average cost value for steel culvert bridges dated 30th June, 2015), it is reasonable to expect a higher saving ratio in the investment cost for other culvert bridges in general.
- In the O&M phase, the elimination of shotcrete activities in the FRP alternative results in a 21% saving ratio due to the relatively high cost of this measure. In this regard, the LCC analysis helps to reveal the saving resulted from FRP culvert during service life, while this is usually neglected in the conventional cost analysis.
- At the end of service life, the disposal cost of the FRP alternative is much lower after taking into account the time value of cash and the longer life span of the FRP bridge, even though the

recycling of FRP material is more expensive than steel.

7 Future study

- In order to have a better control of the deflection in FRP culverts, optimization of the section and use of stiffer fibers such as carbon, in combination with glass fibers to form a stiffer and yet strong FRP skin is suggested. Cross-sectional profile for the FRP culvert structure can also be subjected to optimization to take advantage of geometrical stiffness.
- Design of fiber orientation in the FRP laminate to achieve better material utilization with the help of finite element (FE) modeling.
- Improve the FE modeling method. In this report, the FRP laminate is modeled by solid elements, using equivalent mechanical properties. To study the behavior in more detail, FRP material can be modelled as orthotropic laminate that has a correct stack up with regard to fiber orientation.
- Detailing of the adhesive bond between different segments with regard to strength.

8 Acknowledgment

The authors would like to acknowledge the Swedish Transport Administration for supporting this study and DIAB for collaborating in this project.

Shea D., Vander Pluym J., Eggleston D., Merril M. A., Gregory J., and Bogan A. E. A comparison of the Impacts of Culverts versus Bridges on Stream Habitat and Aquatic Fauna, North Carolina Department of Transportation (Project Number : HWY-2004-08), 2007.

- [7] Available: www.eng.buffalo.edu.
- [8] Available: www.fiberline.com.
- [9] Hexcel, "Honeycomb sandwich design technology," Publ. No. AGU 075B, 2000.
- [10] Safi M. Life-Cycle Costing : Applications and Implementations in Bridge Investment and Management. KTH Royal Institute of Technology, 2013.
- [11] Amanda Sagemo L. S. Comparative study of bridge concepts based on life-cycle cost analysis and life-cycle assessment. Chalmers University of Technology, 2013.
- [12] Haghani R., Yang J. Application of FRP materials for Construction of Culvert Road Bridges- manufacturing and life-cycle cost analysis. Chalmers University of Technology, 2016.

9 References

- [1] Pettersson L., Sundquist H. Design of Soil Steel Composite Bridges, Stockholm, 2010.
- [2] www.batman.vv.se.
- [3] Safi M. LCC Applications for Bridges and Integration with BMS. KTH Royal Institute of Technology, Stockholm, 2012.
- [4] Sundquist H. Soil-Steel Structures: State-of-the-art, Swedish Research, Presentation in NordBalt Seminar, 2007.
- [5] Available: www.cjntech.co.nz/manuals/Find the Answer/#2864.htm.
- [6] Levine J. F., Eads C. B., Cope W. G., Humphries L. F., Bringolf R. B., Lazaro P. R.,



Experimental Study on A GFRP Girder Reinforced with CFRP for Application to Extended Sidewalk

Katsuyoshi Nozaka

Ritsumeikan University, Shiga, Japan

Nobuhiro Hisabe

Mitsubishi Plastics Infratec Co., Ltd, Tokyo, Japan

Masahide Matsumura

Kyoto University, Kyoto, Japan

Contact: k-nozaka@se.ritsumei.ac.jp

Abstract

Although application of Fiber Reinforced Plastic (FRP) to bridge construction has been investigated, design guidelines have not been officially authorized. Thus, it is necessary to investigate the applicability of FRP materials as construction members in each case. In this study, a possibility of adopting a GFRP girder reinforced by CFRP to an extended sidewalk for existing bridges has been investigated. Four-point bending tests were conducted based on the experimental test results of material tests. For the bending test, a stack of four layers of GFRP box section reinforced by a CFRP plate on bottom faces with a GFRP slab was fabricated based on trial design calculations. The strength of the girder was able to be estimated based on the results of material tests, and it was confirmed that deflection requirement was satisfied.

Keywords: GFRP girder; CFRP plate; bending strength; extended side-walk.

1 Introduction

Many existing bridges have been deteriorated by the natural environment effects, such as corrosion. As a new construction material intended to resolve these problems, in recent years the construction industry has turned its attention to fiber reinforced plastic (FRP)^{1,2}.

In addition, there are existing bridges to which a sidewalk must be added or expanded to deal with the change in traffic demand or with seasonal

problems such as snow accumulation³. In such cases, the deck slab of the bridge must be widened, but in many cases, a member that supports the deck slab of the extended part is added to a major structural member such as an existing main girder.

For materials of an extended sidewalk, a light-weight material that is highly corrosion resistant is thought to be appropriate, considering the burden on the substructure of the existing bridge and the ease of its maintenance. Because FRP in particular

is light and heavy machinery is not needed for its execution, it is considered to be highly applicable for extending the sidewalk on existing bridges. Although there are examples of the construction of FRP bridges, there are no design guidelines. To study the possibility of applying FRP as a structural member, it is necessary to clarify its behavior and strength as a component to gather data needed for its design⁴.

In this research, the applicability of CFRP plate reinforced GFRP girders to an extended sidewalk was experimentally examined. The proposed components that support the deck slabs of the extended sidewalk in this study are girders laminated with a box-section GFRP girder. The characteristics of the proposed method, laminating box sections, are the ability to combine girder heights and CFRP reinforcement quantities freely according to the required cross-sectional performance. Using molded materials that are standardized products keeps down costs.

2 Element tests of GFRP girders

In order to clarify the material properties of GFRP girder members (100mm×100mm, thickness 5mm square box section), specimens cut out of a girder member were used to perform tensile tests, compression tests (rectangular section, box section) and local loading tests. Also, flexural load tests of box-section girders were conducted to study the failure mode. The GFRP material used was unidirectional reinforced material.

2.1 Outline of the tests

Figure 1 shows an outline figure of the tensile test specimens. The tensile tests were conducted by bonding steel plates to both ends of the FRP plate, then gripping both ends of the specimen to apply the tensile load. Two kinds of specimens were used.

The dimensions of the fiber direction specimens (A-1 to 3) were 350×40×5mm, those of the direction transverse to the fiber specimens (B-1 to 3) were 100×40×5mm, and six loading tests of each set of three specimens were conducted.

Figure 2 (figure on the left) shows an outline figure of the compression tests of square sections.

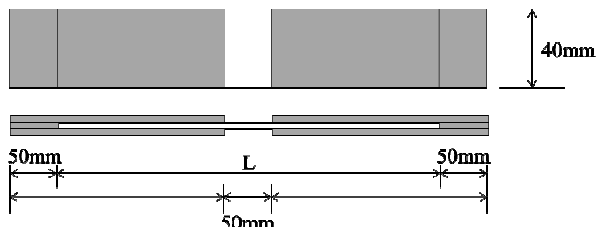


Figure 1. Sketch of tensile test specimen

Thickness 5mm

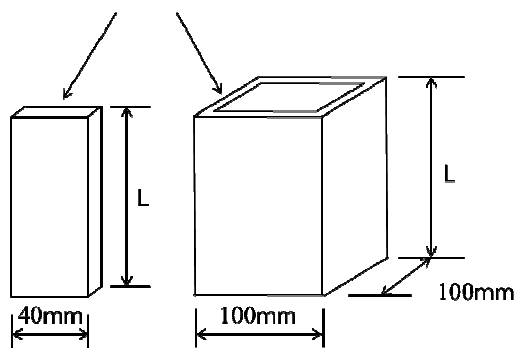


Figure 2. Sketch of compression test specimen

Two kinds of specimens were used, fiber direction (A-1 to 3) and direction transverse to the fiber (B-1 to 3), both with dimensions of 90×40×5mm, and all six specimens were tested.

Figure 2 (figure on the right) is an outline figure of the compression tests of the box section girders. The compression tests of the box sections were conducted to study how the compression behavior of GFRP girder (100mm by 100mm, thickness 5mm square box section) differs from that of the square section girder. There were three kinds of specimens, with height L of 90mm (A-1 to 3), of 180mm (B-1 to 3) and of 270mm (C-1 to 3), and nine tests were carried out using each set of 3 specimens.

Figure 3 is an outline figure of the local loading tests. In the case where flexural load tests of the GFRP girder were conducted, it was anticipated that sinking failure (bearing pressure failure) would occur at the loading location, and without reaching the compression strength or tensile strength, the girder might lose its bearing strength. In advance, the degree of bearing pressure at which sinking failure would occur on a box section was experimentally studied.

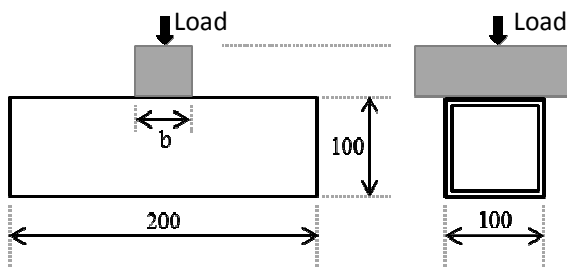


Figure 3. Sketch of local loading test specimen

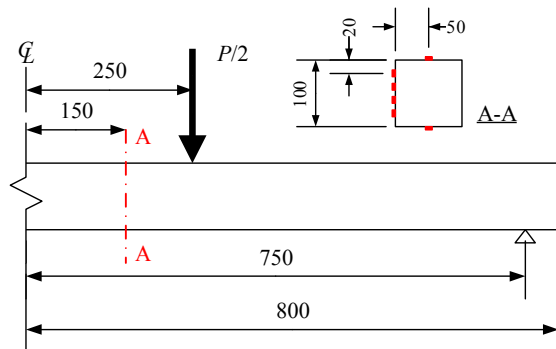


Figure 4. Sketch of Flexural loading test specimen

The specimens used were GFRP girder members with a length of 200mm, and six loading tests of each of the three specimens were conducted at two loading ranges: 50mm (A-1 to 3) and 100mm (B-1 to 3).

The flexural loading test of GFRP girders were conducted using square box-shaped section specimens with dimensions of 100mm by 100mm, thickness of 5mm, and length of 1,600mm. Span length was 1,500mm and uniform bending region was 500mm (Fig. 4).

Strain gauges were applied to three surfaces: the top and bottom surfaces and one side surface. The measurements were done in the uniform bending section in two rows located 150mm to the left and right of the center. On the top and bottom surfaces, one was installed in the center while they were installed at 20mm intervals in the height direction on the side surface, so that strain was measured at six locations on each row for a total of 12 locations. Deflection was measured at one location on the center of the girder.

2.2 Test Results

Table 1. Summary of test results

	A	B	C
tensile test	292	39	—
compression test (square)	252	69	—
compression test (box)	203	164	179
local loading	45	86	—

Table 2. Theoretical buckling strength
(square section)

boundary condition	A (fiber direction)		B (transverse)	
	simple	fix	simple	fix
buckling strength	87.0	347.8	23.1	94.2

Results of material tests (average values) are summarized on Table 1. The values in Table 1 were shown in units of N/mm² unless indicated in the table.

In the results of the tensile and compression tests, results for type A and B are generally within the range of the catalog values. The elastic modulus was computed from the tensile and compression test results, and the average values, 34,000N/mm² and 11,000N/mm² respectively are higher than the catalog values.

Since buckling failure was considered, the buckling strength were computed using the modulus of elasticity obtained from tensile and compression tests (Table 2). In both type A (fiber direction) and type B (direction transverse to the fiber), the buckling strength in a case of simple support was lower than the catalog value. It seems that the actual boundary conditions were nearly fixed boundary conditions.

In the compression test of the box section, scattering of test results was large, and if only the average values (listed in Table 2) are examined, the results varied according to the height of the specimen. When one side of the box section was considered to be the compression plate with simple support on both ends, the buckling strength was approximately 311N/mm², which is larger than the test results. This can be explained by the difference in the failure configuration. It is presumed that when the box section received



Figure 5. Failure mode of flexural test of box section girder

compressive force, out-of-plane deformation near the center of the specimen height was severe, tensile stress occurred at the corners resulting in rupture failure at the corner. This failure mode is also indicated by other researcher⁵.

The local loading test results are averages of values obtained by dividing the maximum load by the section areas in contact with the webs. When type A and type B were compared, the maximum load is almost proportional to the loading width. This shows that the bearing strength is simply dependent on the material strength of the bearing part.

In the case used as the girder, increasing its loading width (lengthening the bearing part) is unrealistic, and in order to use it as a girder, it is necessary to also study reinforcement at the bearing part.

In the flexural loading test of the box-shaped specimen girder, the maximum load at the total of the two loading points was an average value of

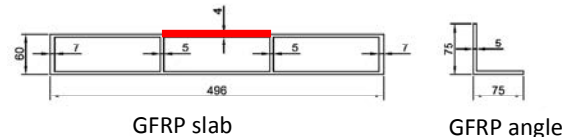


Figure 6. Section of GFRP slab and angle member

40.8kN. As shown in Figure 5, the failure configuration conforms to that of the compression tests of box sections, and on the compressive side of the specimen, the corners cracked, breaking the bonds between the top surface and side surfaces. The theoretical failure load of a GFRP single girder based on the compressive strength of 182N/mm^2 obtained by the compression tests of the box section (average value of A, B, and C) was 41.8kN, which was close to the maximum load of 40.8kN in the experiment.

3 Flexural tests of a GFRP Girder with a GFRP deck slab reinforced with a CFRP plate

3.1 Detail of Specimen

Girder specimens were fabricated by longitudinally laminating GFRP girders in four layers, then applying one high-elasticity CFRP plate with width of 50mm and thickness of 1.2mm (modulus of elasticity=450,000N/mm², tensile strength=1,200N/mm², and volume fraction of fiber: 65 to 70%) to its bottom surface. It was considered to be a composite girder with a GFRP deck slab (material properties of a GFRP box-

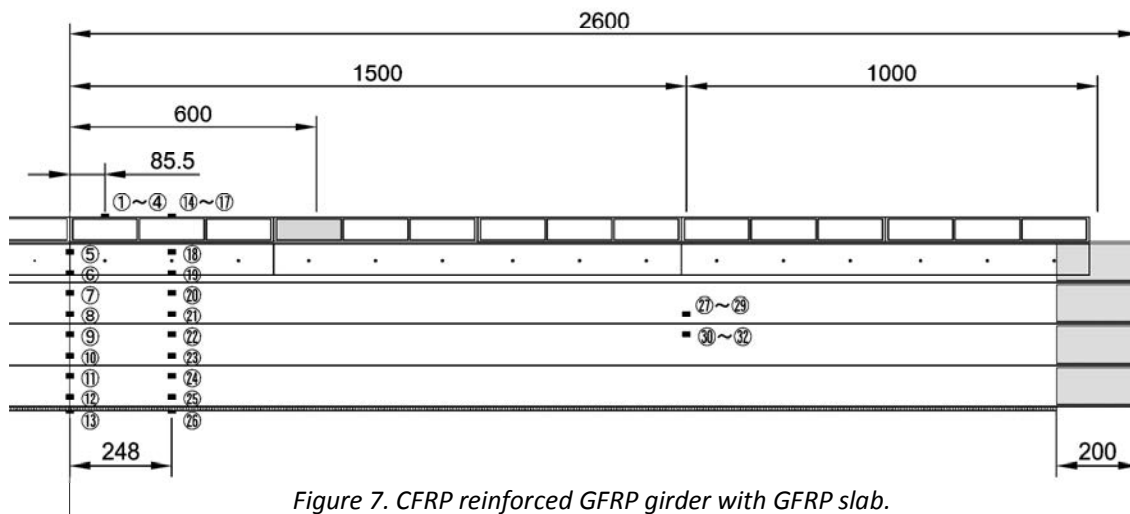


Figure 7. CFRP reinforced GFRP girder with GFRP slab.

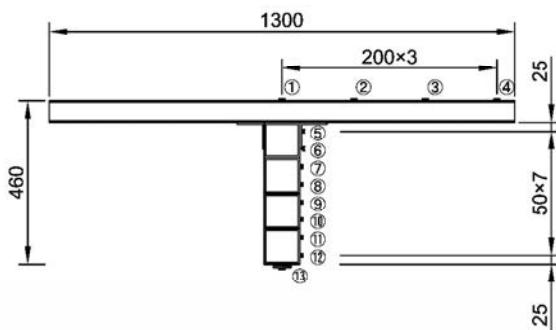


Figure 8. Section of CFRP reinforced GFRP girder with GFRP slab

girder). The laminated GFRP box-section girders and deck slabs were joined using an epoxy adhesive (tensile shear strength of 17.5N/mm^2). And the laminated box-section girder to deck slab connection was formed using both GFRP angle member and blind rivets (shear strength of 5.3kN SS400 steel), strengthening its composite action. The section dimensions of the GFRP deck slab and angle member are shown in Figure 6. The composite action with the deck slab was considered as important in order to restrict failure at corners such as the failure configuration seen in the compression tests and bending tests of the box section shown in Chapter 2.

The specimens had girder length of 5,200mm and span length of 5,000mm. The outline of the specimens is shown in Figure 7, and Figure 8. As shown by Figure 7, the GFRP deck slabs were the members shown in Figure 6 (length 1,300mm = deck slab width) installed in a multiple arrangement in the bridge axis direction. The angle member, GFRP deck slab, and GFRP girder were, in addition to being bonded, connected by blind rivets installed at intervals of about 165mm.

3.2 Loading and measurements

Loading was done as four-point bending loading with a uniform bending region of 1,200mm and a shear span of 1,900mm, using a hydraulic jack (static maximum load of 2,000kN). Because concentrated load was placed on the loading points and support points and because according to the results of local loading tests in Chapter 2, reinforcement was necessary. The places shown by the shading in Figure 7 were filled with non-shrink mortar. And because the loading beam was

narrower than the deck slab, the deck slab was loaded through wooden material (section of $100\text{mm}\times100\text{mm}$, length of 1,300mm).

The measurement was done by measuring the load and stroke from the hydraulic jack, and also the vertical displacement of the bottom surface at the span center and loading points. Also, strain was measured at the locations of the numerals in circles in Figure 7 and Figure 8. From 1 to 26, the normal strain was measured by a single-axis gauge in the bridge axis direction, and from 27 to 32, shear strain was measured by a 3-axis gauge.

3.3 Test results and discussions

3.3.1 Load – deflection curves and failure configuration

Figure 9 shows the load-deflection curves. The blue line is the deflection at the loading point and the yellow line represents the deflection at the center of the span. The red line is the theoretical value when only the flexural deformation at the loading points was considered. The sectional moment of inertia of the section shown in Figure 9 (section of angle member is ignored) is approximately $2.87\times108\text{mm}^4$ and the neutral axis is located at 207.6mm from the top edge (converted to GFRP material $E = 34,000\text{N/mm}^2$). At

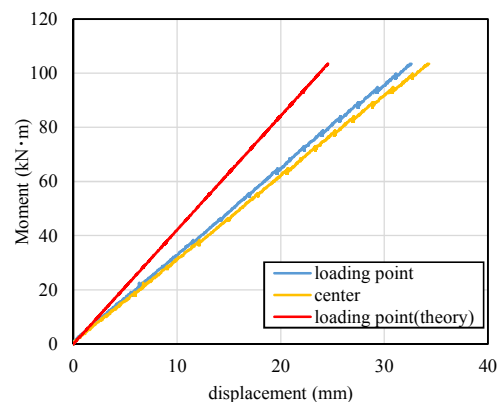


Figure 9. Moment-deflection curve



Figure 10. Failure mode of specimen

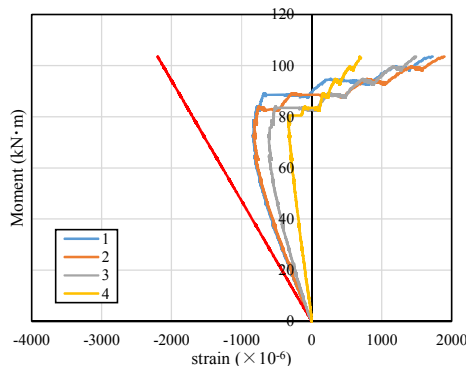


Figure 11. Strain in GFRP slab (at 85.5mm)

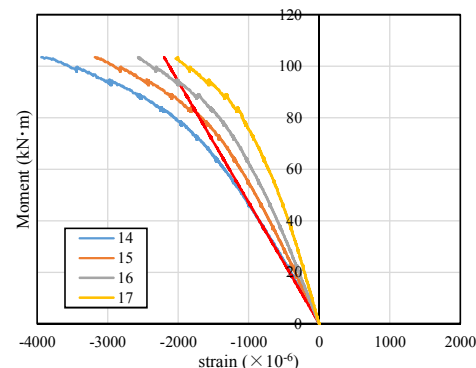


Figure 12. Strain in GFRP slab (at 248mm)

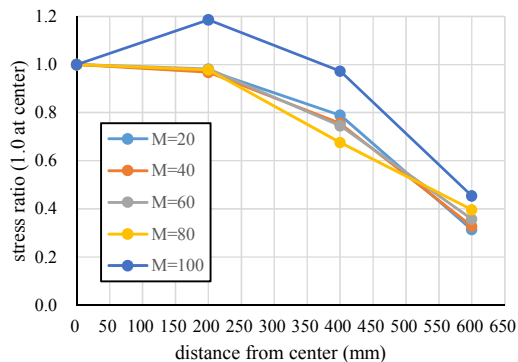


Figure 13. Strain distribution in GFRP slab (at 85.5mm)

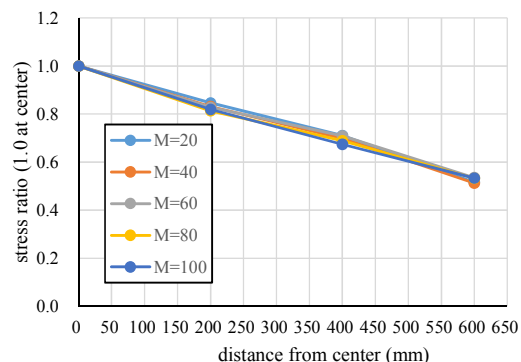


Figure 14. Strain distribution in GFRP slab (at 248mm)

the maximum load (108kN, bending moment = 102kN-m), as shown in Figure 10, the GFRP deck slab buckled, and the graph plots until the maximum load. Figure 9 reveals that the theoretical values are much smaller than the measured values, and that it is necessary to consider the deflection by shear deformation. This point is discussed later.

3.3.2 Strain in the deck slab

Figures 11 and 12 show strain of the GFRP deck slab. The vertical lines show the bending moment (kN-m) that acts on the uniform bending section. Compared with the theoretical value in red line, strain varies width direction because of shear lag. Since measured values are deviated at a location 85.5mm from the loading point, it is thought that out-of-plane deformation is caused due to the deck slab's structural shape.

Figures 13 and 14 show the strain distribution in the width direction at 85.5mm and 248mm from the span center with the value of strain at the

center in the width direction as 1.0. The axis of abscissas is the distance from the center of the width direction. It shows that the distribution at 248mm is linear, and the distribution profile does not change as the bending moment increases, but the distribution at 85.5mm is non-linear, and its distribution profile changes at M=100 kN-m. This is thought to be a result of the fact that because the GFRP deck slab is a single member with three box sections, the distribution profile at 248mm that is the section at its center was relatively stable.

3.3.3 Strain distribution in the girder section

In order to verify if, in the unidirectional fiber reinforced material, which is anisotropic material, the Navier hypothesis of the section can be applied as it is with steel, or in other words, if the linearity of the strain distribution can be used to calculate the stress in the section, the strain distribution in the section is plotted as shown in Figure 15. The axis of ordinates shows the

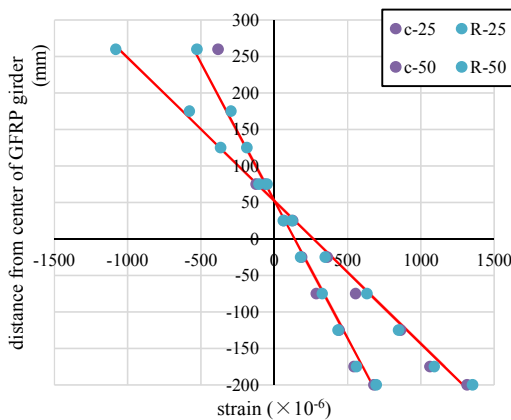


Figure 15. Strain distribution in girder section

distance (upwards as positive) from the center of the GFRP laminated girder (between the 2nd and 3rd layers) and the axis of abscissas represents the strain. The values at the bending moment 25 and 50 kN-m are shown. "C-" in the legend is the value at the near span center (85.5mm), and "R-" is the value at 248mm. The red line is the theoretical value at each bending moment value.

In this figure, the strain distribution in the section is linear excluding the GFRP deck slab portion (particularly, the span center, =85.55m location), confirming that it is possible to also apply the Navier hypothesis to the stress verification.

3.3.4 Calculating the shear modulus of elasticity

The gauge numbers 27 to 29 and 30 to 32 shown in Figure 7 are 3-axis gauges, and the shear strain was calculated. By assuming that the acting shear force is resisted only by the web of the GFRP box section girder, the shear modulus of elasticity was obtained by dividing the shear stress by the measured shear strain, and it was in a range of approximately 3,000 to 3,500 N/mm². Because the catalog value shown in Table 2 did not include the shear modulus of elasticity, to calculate the shear deflection, it was assumed that the shear modulus of elasticity was the minimum value of 3,000 N/mm².

The shear deflection was calculated using the hypothesized shear modulus of elasticity, and Figure 16 shows the deflection at the loading point calculated by summing up the theoretical values of deflection based on the bending

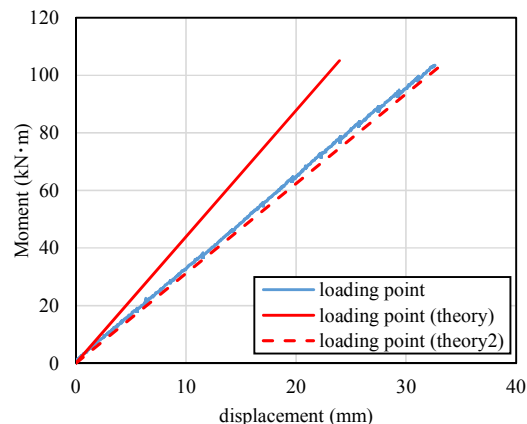


Figure 16. Moment-deflection curve (considering shear deformation)

moment shown in Figure 9. In the figure, to simplify comparison, the deflection at the center span shown in Figure 9 is deleted. From the figure it was assumed that it is possible to generally reproduce the deflection obtained by testing and that it can also be applied to design calculations.

3.3.5 Load bearing capacity

As stated above, the maximum load was governed by buckling of the GFRP deck slab. So the load and bending moment at the time the GFRP deck slab buckles is calculated. The length of one cell of the GFRP deck slab shown in Figure 6 by a red line is about 158mm, and if it is assumed that this part is a structure subject to compression (loading side is a simple support, and the other is free), the buckling stress is obtained as approximately 23.2 N/mm². The Young's modulus used was 11,000 N/mm², which was the value in the direction transverse to the fibers that obtained in Chapter 2. If the acting bending moment at the time this buckling stress is produced is reverse calculated, it is approximately 99 kN-m, and it is possible to roughly predict the maximum bending moment of 102 kN-m obtained from the tests.

It is predicted that the CFRP plate bonded on the tension side will also fail, but if it is presumed that the failure strength of the high-elasticity CFRP plate is 1,200 N/mm², the maximum bending moment will be about 103 kN-m, and although there will be a slight difference, it was predicted that the buckling of the GFRP deck slab governs the load bearing capacity. Because the predicted

failure strength is the catalog value that is the lower limit value of the tensile tests, it can be stated that observed failure configuration at the experimental test was as predicted.

4 Conclusions

This study verified the applicability of a laminated GFRP girder reinforced by a CFRP plate to an extended sidewalk. First element tests of the materials that constitute the GFRP girder were conducted, clarifying the material properties. The element tests were tensile tests, compression tests of rectangular sections and box sections, partial loading tests of box sections, and bending tests of single GFRP girders. Based on the results of the element tests, a trial design was performed and the main girder section dimensions attached to the deck slab were decided. Based on the section dimensions that were decided, specimens were prepared and flexural load tests conducted, verifying that the specified bearing capacity was obtained. The following are the major conclusions obtained.

- 1) According to the results of the element tests, at the dimensions used here, if a GFRP box section is subjected to compressive axial force, failure of the corners determines the bearing capacity. Thus it is more rational to design it as a composite section with the deck slab linked on the compression side of the GFRP box section.
- 2) The flexural load tests of the GFRP girder with deck slab attached confirmed that it has the stipulated flexural capacity, and also confirmed that it is possible to specify the bearing capacity of the section based on the local buckling strength of the GFRP deck slab.

In the future, a prototype bridge will be made using CFRP reinforced GFRP girders and its performance will be verified in order to prepare for its practical application to actual bridges. It is also predicted that when it is applied to an actual bridge, the span lengths will vary, so this will be dealt with by revising the values for the GFRP box section girder that is laminated. And because, as the results of these tests have shown, at bearing

locations and others subjected to concentrated load, strength is required inside the box section, end reinforcing materials that will also function as supports will be studied.

5 Acknowledgements

The authors wish to express their gratitude to Omori Masakazu who was then at Ritsumeikan University for his assistance with the studies performed during this research project.

6 References

- [1] Japan Society of Civil Engineers *FRP Bridges Technologies and their Future*, Structural Engineering Series 14. Tokyo; 2004.
- [2] Japan Society of Civil Engineers *Advanced Technologies of Joining for FRP Structures and FRP Bonding for Steel Structures*, Hybrid Structure Reports 09. Tokyo; 2013.
- [3] Kakuma K., Okada S, Kubo K., and Matsui S. Study on load carrying performance of FRP slabs for sidewalk widening of narrow highway bridges. *Journal of Structural Engineering*. 2014; 60A: 1150-1158.
- [4] Correia J. R., Branco F. A., Silva N. M. F., Camotim D., and Silvestre N. First-order, buckling and post-buckling behaviour of GFRP pultruded beams Part 1: Experimental study. *Computers and Structures*. 2011; 89: 2052-2064.
- [5] Sakuraba, H., Matsumoto, T., and Hayashikawa, T. Flexural Behavior of CFRP Box Beams with Different Laminate Structures. *Journal of Japan Society of Civil Engineers*. 2012; A1 68(1): 73-87.



KuBAal - Bocholt (Germany) – Design of a GFRP footbridge as part of an urban development

Sarah Hübner; Katrin Baumann

Arup Germany, Düsseldorf

Edwin Thie

Arup Netherlands, Amsterdam

Contact: sarah.huebner@arup.com

Abstract

This paper describes the structure of a weathering steel footbridge with a GFRP deck, as part of a larger redevelopment of a former industrial area in the City of Bocholt - KuBAal.

In the recent past, the requirements on the design of footbridges regarding economic design in combination with architecture, especially in urban developments with limited budget of local authorities have increased. It is the challenge of the engineering process to explore fitting solutions to meet these requirements.

The footbridge in the KubAal follows the chosen design concept of a low maintenance bridge by the use of appropriate materials, such as weathering steel for the main steel structure and GFRP elements for the bridge deck, and an aesthetically pleasing appearance. The structure will blend into the industrial surroundings and be much more than a mere connection, it is also a public space.

Keywords: Footbridge, steel structure, weathering steel, GFRP composite, vibrations, light structure, economic structures, sustainability

1 Introduction

The city of Bocholt has a former industrial area of 25 ha which will be restructured to an urban and cultural district for people to work, live, and explore. SeARCH architects in collaboration with landscape architects B+B were chosen to develop a concept for the renovation of the public space. As a result, four footbridges are planned not only to connect the two parts of the area which are separated by the river Aa, but also to be part of the new urban development.

In the centre of the former industrial area the river Aa is part of the re-cultivation. Hence, the connecting bridges are not only an architectural statement, but also show the transition from the former industrial origin to the new cultural urban district. The design of the bridges is chosen to meet the idea of the old and the new. Three of the four bridges will be newly designed whereas one former railroad bridge will be refurbished for the use as a pedestrian bridge.

The following figures show an overview of the area with the planned bridges.

The biggest of the four bridges is the "Podiumbrücke". It is not only a footbridge that connects the two river sides but also a location for events such as the "Regionale 2016". Therefore,

special comfort requirements on vibration have to be considered.

The following sections provide details regarding the structural design of the "Podiumbrücke".



Figure 1. Overview of the restructured area of KuBAal @ City of Bocholt



Figure 2. Visualisation of "Podiumbrücke" ©SeARCH

2 Structural Design

The "Podiumbrücke" with a span of 47 m and a width of 14 m is the biggest of the four bridges. Two main girders with a length of 47 m and a variable height between 1.6 m and 2.6 m are designed as complex welded box sections in

weathering steel that also serves as parapets for safe access.

The deck of the footbridge will be made of lightweight GFRP (Glass-Fibre Reinforced Plastic) elements that will be adhesively bonded on cross girders, which are attached to the main girder every 2.35 m. The bridge will have an integral structural system where each member will be part

of the structural system. This allows for a very material-efficient design.

2.1 Design Concept

The design of the footbridge is based on the Eurocode 3: DIN EN 1993-2: Steel Bridges [1]. The design and assessment is analysed with Sofistik, which is a finite element program specialised in the structural design of three-dimensional structures. The bridge is completely modelled in 3D including all structural parts.

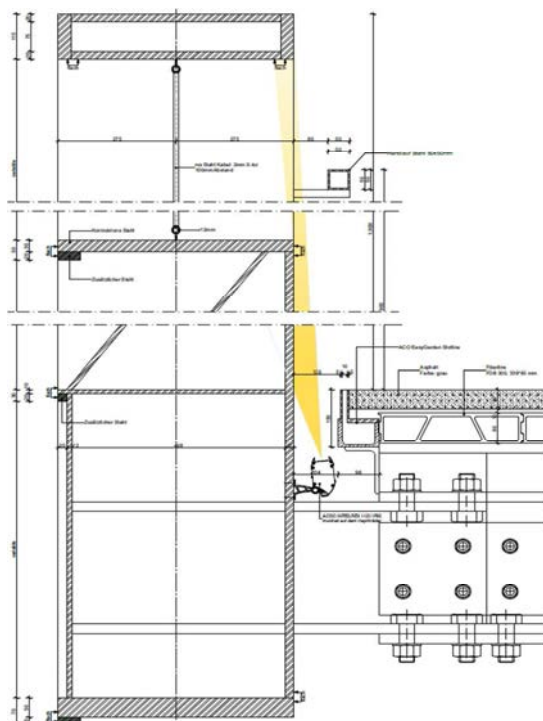


Figure 3. Section through the main girder
©SeARCH

2.2 Main Girders

2.2.1 Material

The main girders are made of weathering steel.

According to DIN EN 10020, 1989 [2], weathering steel is part of the group of stainless steel.

The obvious difference of weathering steel and normal construction steel is that weathering steel is mainly used unprotected, i.e. without any coating. Directly exposed to weather conditions, the steel corrodes and forms a protective rust

layer, resulting in a natural rusty colouring and its special appealing aesthetic.

Compared to normal construction steel, weathering steel has a much higher resistance to atmospheric corrosion. This means that after a few years the process of corrosion has nearly stopped and can be neglected.

Although material costs for weathering steel might be slightly higher than for normal construction steel its use for steel constructions has big economic benefits: No costs for anticorrosive coating and all associated work over the life cycle of the structure which is a 100 years.

Since no coating work is required on site construction time can be minimised.

Another positive effect is the environmental benefit: Pollution of air and water, which emerge from the coating process, the removal of the coating and the recycling process, can be avoided. In addition, the steel can be fully recycled at the end of life, reducing waste and promoting a circular economy.

To ensure that the corrosion process stagnates until it nearly stops, construction details have to be designed in such way that the structure is not permanently wet and that water due to rain can drain.



Figure 4. Architectural visualisation of weathering steel main girder ©SeARCH

This and further information of weathering steel have been e.g. published by the Stahl-Informations-Zentrum [3].

Since initial corrosion of weathering steel in the first few years has to be expected a reduced

thickness of the steel structure is taken into account for the FE analysis. For each steel face exposed to the environment a corrosion of 1 mm is assumed.

2.2.2 Stability

The stability checks are executed as part of the FEM analysis.

As first step, a buckling mode shape analysis of the steel structure is carried out in order to identify the critical areas of the bridge structure in terms of stability, including global and local buckling modes. This step is important to understand how the buckling modes look like in order to apply imperfections accordingly in the next step.

As second step, these critical areas are investigated more in depth. The simple details of the structure (e.g.: rectangular sheets) are designed according to DIN EN 1993-1-5 [4], chapter 10 by using the reduced stress method. This method may be used to determine the stress

limit. It is used to reduce the elastic stresses in every part of the section to a local buckling resistance.

Details with more complex geometry are modelled as FEM model and an initial imperfection according to DIN EN 1993-1-5 [4] is applied. This local model is analysed via 3rd order theory and the resulting stress are checked against the design value.

Finally, in a last step, a 3rd order analysis of the whole structure is carried out. This is a geometric non-linear calculation which considers the actual deformed shape of the structure. For this analysis no initial imperfection is taken into account since the system is deforming already due to the applied loads. The comparison of the stresses in the main girders between linear and 3rd order analysis shows a P-delta magnification is only 1%. This verifies that overall stability of the bridge is not critical.

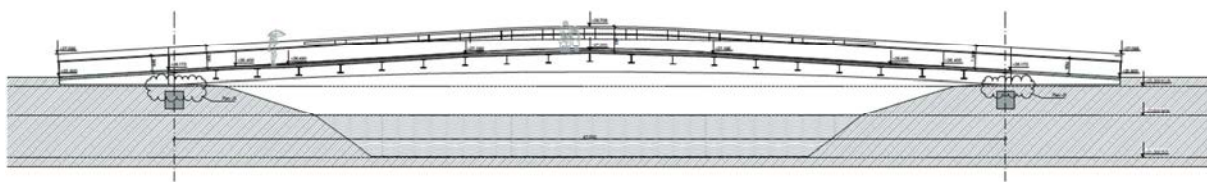


Figure 5. Longitudinal section through "Podiumbrücke" ©SeARCH

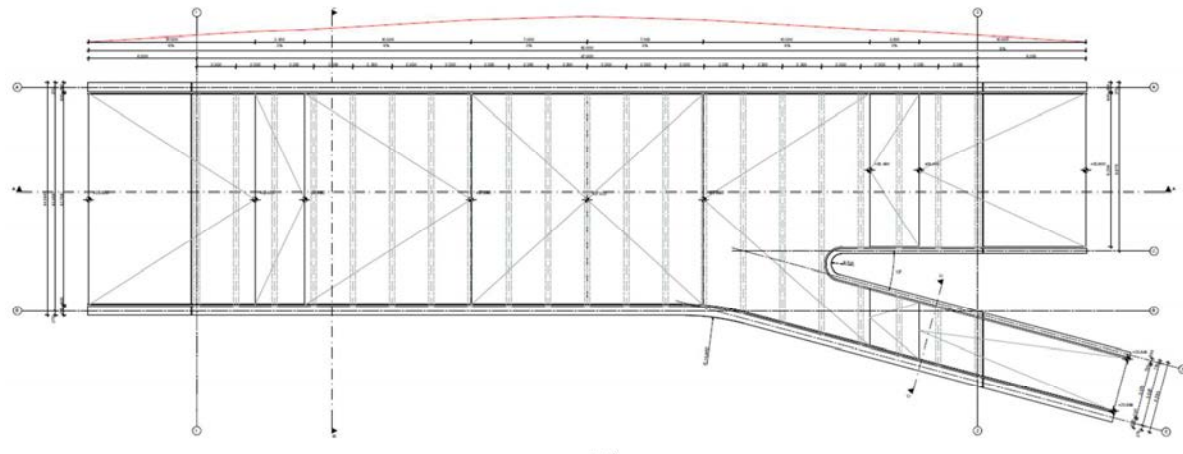


Figure 6. Top view of "Podiumbrücke" ©SeARCH

2.3 GFRP Composite Deck

2.3.1 General

Glass-fibre reinforced plastic (GFRP) or Fiberglass is a composite material consisting of two components: glass fibres and polyester or epoxy resin. Both components on their own would not be useful for construction, but put together generate an ideal material behaviour.

GFRP can be divided into two groups: composites with short fibre reinforcement and with long, continuous fibres.

Short fibre reinforced composites are typically used for casting or extrusions and long fibre reinforced composites generally for big elements in shipbuilding or air craft industry. The fibres mainly bear tensile and compression loads, while the matrix, e.g. epoxy bears shear forces.

The fundamental advantage of a composite material is the reduction of weight in comparison to steel or aluminium. The base material is light and can be optimised by choosing the material combination and the direction of the fibre.

Furthermore, in comparison with the common composite material like concrete, fibre reinforced composites have advantages in corrosion, chemical resistance and electrical and thermal insulation.

Over the last decades composite materials have become more and more popular and their advantages and durability are much valued. Research and product development have constantly improved material properties. Improved FEM tool now allow for modelling with more realistic material behaviour and design safety.

2.3.1 Structural Design

FBD 300 GFRP composite extruded planks are used for the design of the bridge deck. The profile consists of prismatic hollow section which is 333 mm wide and 80 mm high. The segments are placed next to each other to form a continuously closed area over the bridge. On the top surface a GFRP plate with 10 mm thickness will be adhesively bonded on the elements. It serves as a

protection layer since a 50 mm asphalt layer will be applied on top of the deck. The later removal of the asphalt would mean mechanical damage to the top layer. Thus, it is not utilised as structural element but merely serves as protective layer and interconnection of the FBD 300 elements.

As the deck profile FBD 300 is not yet covered by codes or technical approval in Germany, the design is done following a recommendation by the BÜV, a technical working group of checking engineers [5].

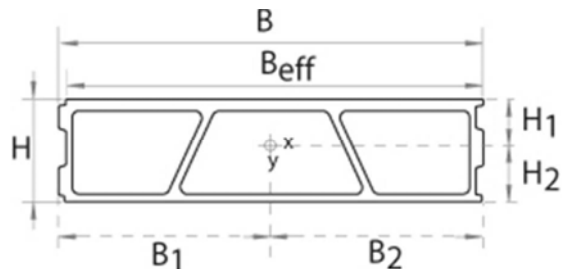


Figure 7. GFRP section FBD300 © Fiberline

Table 1. Average values for local analysis-flanges acc. to [6]

Modulus-axial Tension E_{ts}	MPa	27000
Modulus-axial Compression E_{cx}	MPa	27000
Modulus-transverse Tension E_{ty}	MPa	14000
Modulus-transverse Compression E_{cy}	MPa	14000
Strength-axial Flexural f_{fx}^*	MPa	300
In-plane shear modulus G	MPa	3000

Table 2. Average values for local analysis-webs acc. to [6]

Modulus-axial Tension E_{ts}	MPa	20000
Modulus-axial Compression E_{cx}	MPa	15000
Modulus-transverse Tension E_{ty}	MPa	18000
Modulus-transverse Compression E_{cy}	MPa	18000
In-plane shear strength tm^*	MPa	61
In-plane shear modulus G	MPa	3000

*5 % fractile characteristic value

Former test reports [6] and [7], in which material properties have been investigated, build the basis of the design calculation.

The design is based on the ultimate limit strength and serviceability limit. In the following the ultimate limit strength design is explained conceptually. For the ULS following requirement must be fulfilled:

$$E_d(t_a) \leq R_d(t_a) \quad (1)$$

$$R_d(t_a) = \frac{R_k}{\gamma_M \cdot A_1 \cdot A_2 \cdot A_3} \quad (2)$$

$E_d(t_a)$: action design value for the accumulated action period t_a

R_k : characteristic material resistance

γ_M : partial safety factor for material

A_1 : factor of influence due to action period

A_2 : factor of influence due to chemical impact

A_3 : factor of influence due to temperature

This means that the load bearing capacity of GFRP is depending on the accumulated time a load is present, as well as on chemical impact and ambient temperature.

For each class of action period ("Klasse der Lasteinwirkungsdauer" - KLED) a separate check has to be performed:

KLED permanent: $1,35 \cdot DL$

KLED short: $1,35 \cdot DL + 1,35 \cdot LL$

According to table 6-2 [5] the bridge can be classified as "Wirtschaftsweg", i.e. agricultural road resulting in the KLED of traffic loads is "short". Since the live loads are very high compared to the bridge self-weight only the design check for KLED "short" is performed.

The deck elements are subjected to bending and shear forces. Therefore, the following design criterion has to be met:

$$\left(\frac{\sigma_{xd}}{f_x} \right)^2 + \left(\frac{\tau_{xd}}{f_{txy}} \right)^2 \leq 1 \quad (3)$$

To accelerate the construction process, the deck profile FBD 300 will be fully adhesively bonded with Sikadur 30 to the steel floor beams. However, for the global design of the steel structure the composite action of the GFRP deck is not taken into account. As a consequence, lateral stiffness will be ensured by the steel bracing and not by the deck element.

Nevertheless, due to the adhesive bonding the GFRP deck will be subjected to restrained forces from the global structural system. For example, these forces are caused by different thermal expansion of steel and GFRP and also since the GFRP deck is not in the neutral axis of the overall cross section. It must be guaranteed that the adhesive layer between steel and GFRP can bear the induced shear forces.

To simulate the composite behaviour between the GFRP and the steel structure, the deck is implemented as shell elements into the global 3D model. To cover the adhesive joint, spring elements are adjusted with the stiffness of the chosen adhesive, an epoxy grout Sikadur 30. Following figures show the shear forces in longitudinal and transverse direction that occur due to vertical loading.

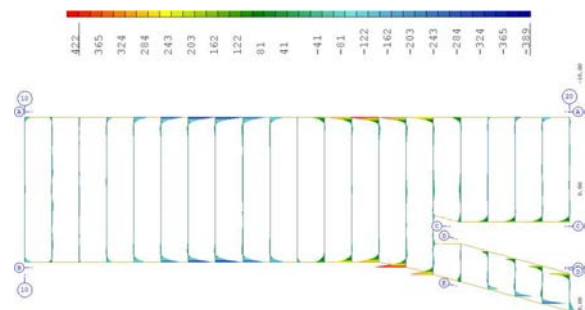


Figure 8. Shear forces in the adhesive layer - longitudinal direction

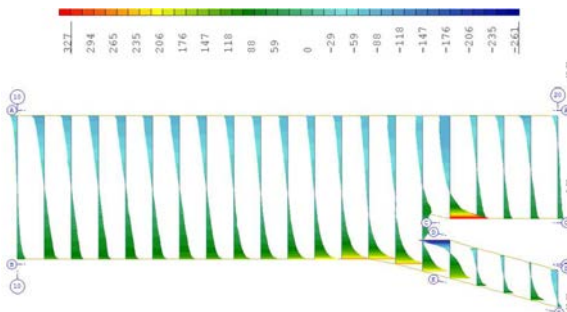


Figure 9. Shear forces in the adhesive layer - transverse direction

Since the epoxy grout shows elastic behaviour, the adhesive layer needs to be designed for the highest stress peaks. The decisive values occur near the main girder – note that the GFRP deck is only adhesively bonded to the floor beams, not directly to the main girders. Even though the design capacity of the adhesive is comparatively low, the maximum stress due to dead load, live load and temperature can still be accommodated by the adhesive.

2.4 Vibrations

2.4.1 General

Vibrations have become an important issue in footbridge design in the recent years.

Developments and innovations in material properties, architectural design, design methods and building techniques have led to bridges which are lighter and more slender. These bridges tend to be more susceptible to dynamic loading, which will be reflected by the vibration behaviour, in particular for structures with high ratio between dead load and life load.

The common dynamic loading results from the pedestrian traffic. Therefore, it is important that footbridges are not only designed for static loads but also for dynamic loads.

The pace of the pedestrian affects significantly the vibration behaviour of the bridge. In some cases, when the walking pace approaches the natural frequency of the bridge, these vibrations can attain high proportions. In that case pedestrian can feel uncomfortable or even unsafe.

Several researches have been done to evaluate recommendations on limits for vibrations and acceleration [8] and [9].

2.4.2 Critical frequencies

In terms of national codes, vibration is still a developing field. Some codes refer to this topic, but only provide recommendations.

EN 1990: 2002 [10] defines comfort criteria in terms of maximum acceptable acceleration and values of frequencies, for which a detail comfort criteria design should be done.

Table 3. Fundamental frequencies for comfort criteria assessment [10]

Vertical vibrations	< 5 Hz
Horizontal and torsional vibrations	< 2.5 Hz

Table 4. Recommended maximum values of the acceleration [10]

Vertical vibrations	0.7 m/s ²
Horizontal vibrations (normal use)	0.2 m/s ²
Horizontal vibrations (crowd conditions)	0.4 m/s ²

Table 5. Critical range of natural frequencies [8]

Vertical and longitudinal vibration	1.25 Hz < f _i < 2.3 Hz
Lateral vibration	0.5 Hz < f _i < 1.2 Hz
Vertical vibration 2 nd harmony	1.25 Hz < f _i < 4.6 Hz

The dynamic design of the “Podiumbrücke” leads to the following frequencies:

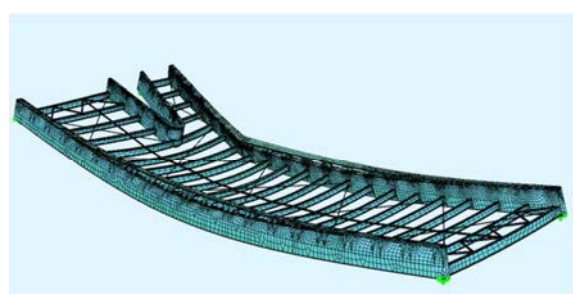


Figure 10. 1st natural frequency 1,6Hz (vertical)

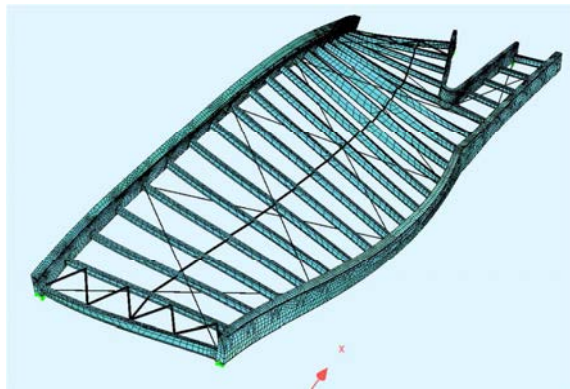


Figure 11. 2nd natural frequency 2,4Hz (torsional)

First and second natural frequencies are in the critical range as defined in [8] and [10].

Damping effects were neglected, which makes it difficult to rely on the calculated values. However, it can be assumed, that according to the low frequency, the bridge will be susceptible for vibration. EN 1990:2002 [10] states: "The data used in the calculations, and therefore the results, are subject to very high uncertainties. When the comfort criteria are not satisfied ..., it may be necessary to make provision in the design for the possible installation of dampers in the structure after its completion".

After consultation with a company specialised in vibration control, it has been decided to make provision for dampers and conduct testing of the dynamic behaviour of the bridge when construction work is finished. After sufficient results will be available it will be decided if the installation of dampers will be necessary. Loads due to dampers are taken into account in the bridge design preventively.

3 Conclusions

The bridge presented in this paper is an excellent innovative and sustainable solution for the KuBAal area as it combines appealing architecture with economic issues.

From an architectural point of view, the bridge fits very well in the industrial surroundings and will connect the redeveloped public areas on both sides of the river Aa.

The materials that are chosen meet not only the requirements of architecture but also of economy and cost effectiveness.

Weathering steel that will be used for the main steel structure requires no protective coating against corrosion as normal steel does. Therefore, there will be no costs for anticorrosive coating and all associated work, maintenance work and environmental impact is reduced.

The use of a GFRP (Glass-Fibre Reinforced Plastic) composite bridge deck follows the chosen design concept of a low maintenance bridge. This material has nearly the same load bearing capacity as steel, but is much lighter and corrosion resistant.

4 References

- [1] DIN EN 1993-2: Design of Steel structures – Part 2: Steel bridges, 2010
- [2] DIN EN 10020: Definition and classification of grades of steel, 2000
- [3] Merkblatt 434 "Wetterfester Baustahl", Issue 2004, Stahl-Informations-Zentrum, Düsseldorf
- [4] DIN EN 1993-1-5: Design of steel structures–Part 1-5: Plated structural elements, 2010
- [5] BÜV e.V.: Tragende Kunststoffbauteile. Entwurf – Bemessung – Konstruktion. Springer Viehweg, Wiesbaden, 2014
- [6] Fiberline Composites: FBD300 – Test Report. Fiberline Composites A/S, Middelfart (Denmark), 24.11.2008
- [7] KnippersHelbig: Gutachten zur Zustimmung im Einzelfall für die Anwendung von glasfaserverstärktem Kunststoff (GFK) und Epoxidharzklebstoff, 2007
- [8] JRC Scientific and Technical Reports: Design of Lightweight Footbridges for Human Induced Vibrations, 2009
- [9] Lemke Roos, Arup, TU Delft: Human Induced Vibrations on Footbridges, 2009
- [10] DIN EN 1990: Basis of structural design, 2002